Supplementary Information

Molecular Engineering of Asymmetric Aza-BODIPY Dyes for High-Performance Phototherapy

Yuting Wang [†a,b], You Dou [†b], Xiaofang Guan [†b], Panxing Qiu [†b], Wenjun Zhang [a], Ziyang Hou [a], Junhua Zhang [b], Liying Xu[*d], Ci Zhao[*c], Yao Sun*[b], Jun Li *[a]

a. College of Chemistry, Huazhong Agricultural University, Wuhan, 430070, China.

b. College of Biomedicine and Health, Huazhong Agricultural University, Wuhan, 430070, China.

c. Center of Oncology, Renmin Hospital of Wuhan University, Wuhan, 430060, China.

d. Department of Radiology, Zhongnan Hospital of Wuhan University, Wuhan, 430071, China.

Table of Contents

1. Materials and instrumentation

1.1 Materials. All chemicals were purchased from commercial sources. RPMI-1640, and fetal bovine serum (FBS) were purchased from Gibco (Australia). 20% intralipid, 3-(4, 5-dimethylthiazol-2-yl)-2, 5-diphenyltetrazolium bromide (MTT), 2',7'-dichlorofluorescein diacetate (DCFH-DA), PBS, 2,2,6,6-tetramethylpiperidine (TEMPO), 5,5-dimethyl-1-pyrroline-Noxide (DMPO), deoxyribonucleic acid sodium salt from calf thymus (ctDNA) were purchased from Sigma-Aldrich (Poole, UK). RNaseA was purchased from Thermo Fisher Scientific (USA).

1.2 Instrumentation. The ^{1}H and ^{13}C NMR spectra were acquired on a Bruker 400 MHz magnetic resonance spectrometer. Data for ^{1}H NMR spectra are reported as follows: chemical shifts are reported as δ in units of parts per million (ppm) relative to chloroform-*d* (δ 7.26, s), acetonitrile-d_3 (δ 1.94, s), methanol-d_4 (δ 3.31, s); multiplicities are reported as: s (singlet), d (doublet), t (triplet), q (quartet), dd (doublet of doublets), m (multiplet), or br (broadened); coupling constants are reported as a J value in Hertz (Hz); the number of protons (n) for a given resonance is indicated nH, and based on the spectral integration values. ESI-TOF-MS was recorded with a Micromass Quattro II triple-quadrupole mass spectrometer or Synapt G2-Si mass spectrometer using electrospray ionization with a MassLynx operating system (Waters, USA). UV-Vis absorbance was recorded on a PekinElmer Lambda 25 UV-Vis spectrophotometer. Absorption spectra were measured on a UV-vis-NIR spectrophotometer (Shimadzu UV-3600, Japan). Fluorescence spectra were measured on a Fluorolog-3 spectrofluorometer (Horiba Jobin Yvon, France) and the fluorescence emitting within the NIR-II region was measured by a Cary Eclipse fluorophotometer. The NIR-II *in vivo*

system was purchased from Suzhou NIR-Optics Technologies Co., Ltd. NIR-II fluorescence spectra were recorded on an Applied NanoFluorescence spectrometer at room temperature with an excitation laser source of 808 nm. Cellular NIR-II fluorescence images were captured by a NIR-II fluorescence microscope (Suzhou NIR-Optics, China). Other cellular images were captured on an inverted fluorescence microscope (Zeiss Fluorescence Microscope, Germany). The laser of 808 nm wavelength was purchased from Beijing Hi-Tech Optoelectronic (China). Electron paramagnetic resonance (EPR) spectra were trapped by Electron Paramagnetic Resonance A300 (Bruker, German). Flow cytometry was performed on Fortessa X20 (BD Biosciences, USA).

2. Experimental details

2.1 Absorption and photoluminescence excitation (PLE) spectral studies

The UV-Vis-NIR absorbance spectrum of **BT** and **BT-4** were recorded on a PerkinElmer Lambda 25 UV-Vis spectrophotometer. PLE spectra of **BT** and **BT-4** solutions were obtained using an Applied Nano Fluorescence spectrometer.

2.2 Photostability tests

BT, BT-4 and ICG (50 μM) in DMSO were prepared. The photostability of **BT, BT-4** and ICG was investigated by recording the NIR-II fluorescence images after 808 nm laser illumination (1.0 W cm^{-2}) for various time (0, 5, 10, 15, 20, 25 and 30 min). The obtained images were analyzed by Origin and ImageJ software.

2.3 Anti-fluorescence quenching tests

BT and **BT-4** (10 μM) in DMSO/toluene mixture of different volume ratios were prepared. The NIR-II fluorescence images were obtained and analyzed by Origin and ImageJ software.

2.4 Anti-ROS quenching tests

The ROS generation capacity of **BT** and **BT-4** were evaluated using a ROS indicator DCFH-DA.[S1] DCFH-DA was dissolved in DMSO (1.0 mM, 0.8 mL) and mixed with NaOH (0.01 M, 2 mL) to deacetylate into DCFH. The DCFH (20 μM) obtained in this way was added into a different DMSO/H_2O of mixtures of **BT** and **BT-4** (5 μM). Then the mixtures were irradiated with 808 nm laser for 30 s. The fluorescent spectra of DCF (λ_{ex} = 488 nm, λ_{em} = 525 nm) were recorded.

2.5 The ROS penetration depths measurement

To examine the tissue penetration depth response of and **BT-4**, biological tissue was simulated using 1% intralipid (5 mL of 20% adipose lactide mixed with 100 mL of water). A 96 well plates were filled with a solution of DCFH treated with and **BT-4** (10 μM) in DMF. Petri dishes were filled with different volumes of fat, which approximated the wavelength dependence of light scattering in biological tissue. The depth of the capillary is calculated from the area of the petri dish. Place the culture dish on the top of 96 well plate, and then irradiated with 808 nm laser for 3 min to obtain fluorescence image, and the images were analyzed by ImageJ software.

2.6 Detection of ROS types

2.6.1 Singlet oxygen ($^1O_2$) detection

1,3-Diphenylisobenzofuran (DPBF) is commonly used as a $^1O_2$ indicator. Here, DPBF (2 μL, 2 mg mL^{-1}) in DMF solution was added to the 300 μL DMF solution containing **BT-4** (10 μM), and then the UV-Vis absorption spectra were obtained after 808 nm laser irradiation (1.0 W cm^{-2}) at different time points. The $^1O_2$ production was measured by the absorbance drop of DPBF at 410 nm.

2.6.2 Hydroxyl radical (•OH) detection

To investigate the •OH generation capability of **BT-4** (10 μM), Hydroxyphenyl Fluorescein (HPF) was employed as an indicator, which can be oxidized and degraded by •OH. HPF (100 μM) in DMSO solution was added to the 300 μL DMF solution containing **BT-4** (10 μM), then, fluorescence spectra (excited at 490 nm) were obtained after 808 nm laser irradiation (1.0 W cm^{-2}) at different time points. The •OH production was measured by the increase in fluorescence intensity at 515 nm.

2.6.3 Superoxide anion radical ($•O_2^-$) detection

Dihydrorhodamine 123 (DHR123) is commonly used as a $•O_2^-$ indicator. DHR123 (100 μM) in DMSO solution was added to the 300 μL DMF solution containing **BT-4** (10 μM), and then fluorescence spectra (excited at 488 nm) were obtained after 808 nm laser irradiation (1.0 W cm^{-2}) at different time points. The $•O_2^-$ production was measured by the increase in fluorescence intensity at 525 nm.

2.6.4 Further verification via Electron paramagnetic resonance (EPR)

EPR was performed to monitor the generation of ROS by using 2,2,6,6-Tetramethylpiperidinooxy (TEMPO) as the $^1O_2$ indicator and 5,5-Dimethyl-1-pyrrolineN-oxide (DMPO) as the •OH and $•O_2^-$ indicator. Briefly, DMSO (100 μL) containing **BT-4** (10 μM) was irradiated with or without 808 nm laser irradiation (1.0 W cm^{-2}) for 5 min, and then added with TEMPO (1 μL, 20 mM) or DMPO (1 μL, 20 mM) and into the above solutions for EPR measure. The obtained images were processed using Origin software.

2.7 Photo and Photothermal Stability Tests *In Vitro.*

2.7.1 The measurements of the photothermal stability of BT-4.

The **BT-4** solution (20 μM) was irradiated with 808 nm laser (1.0 W cm^{-2}) for 5 min and then naturally cooled for 5 min. The temperatures of five heating-cooling cycles were recorded using an infrared thermal imaging camera.

2.7.2 The measurements of the photothermal conversion efficiency (η) of BT-4.

The photothermal conversion efficiency (η) was calculated by following equations: τ_s is the system time constant of the sample. T_{max} (or T_{sur}) is the equilibrium temperature (or ambient temperature), I is the incident laser power (I = 1.0 W cm^{-2}), A_{808} is the sample absorbance at 808 nm.

$$\eta = \frac{\mathrm{hA}(T_{max}-\Delta T_{sur})-Q_0}{I\left(1-10^{-A_{808}}\right)} \quad (1)$$

$$\mathrm{hA} = \frac{\sum_i m_i C_{p,i}}{\tau_s} \quad (2)$$

$$\tau_s = \frac{\mathrm{t}}{-\ln\theta} = \frac{\mathrm{t}}{\ln\left(\frac{\mathrm{T}-\mathrm{T_{sur}}}{\mathrm{T_{max}}-\mathrm{T_{sur}}}\right)} \quad (3)$$

2.8 Interaction with ctDNA

Deoxyribonucleic acid sodium salt 5 mg was dissolved in 5 mL high purity water. **BT-4** dissolved in the 5 mM Tris-HCl buffer solution (pH = 7.2) with 1% DMSO. Titration of ctDNA (0-0.05 mM) into **BT-4** (20 μM) was monitored by UV-vis spectroscopy, respectively.

2.9 Cytotoxicity Assay

4T1 cell lines were seeded in 96-well plates (4×10^3cells in each well) and incubated in a 37°C cell incubator for 24 h. Then, the DMEM medium was replaced with different concentrations of **BT-4** and ICG (1% DMSO, *v*%) in the medium without FBS for 12 h, and the cells in the plates were irradiated with or without 808 nm laser (1.0 W cm^{-2}) for 5 min each (replaced with fresh culture medium before irradiation). After incubation for another 24 h, added MTT solution (5 mg/mL, 10 μL) in each well, and the cells were incubated for another 4 h. The formed formazan crystals were dissolved by DMSO (100 μL per well) and the absorbance at 570 nm was measured using a microplate reader.

2.10 Mechanism studies of cellular uptake

4T1 cells were seeded on confocal dishes (5×10^4 cells/dish). Cells were divided into seven groups and pretreated with (1) **BT-4** (10 μM, 1% DMSO, v%) at 37°C; (2) **BT-4** (10 μM, 1% DMSO, v%) containing 2-Deoxy-D-glucose (50 mM) and oligomycin (5 μM) at 37°C; (3) **BT-4** (10 μM, 1% DMSO, v%) containing NH_4Cl (50 mM) at 37°C; (4) **BT-4** (10 μM, 1% DMSO, v%) containing triethylamine (1 mM) at 37°C; (5) **BT-4** (10 μM, 1% DMSO, v%) containing chloroquine (100 μM) at 37°C; and (6) **BT-4** (10 μM, 1% DMSO, v%) containing Methyl-β-cyclodextrin (M-βCD) (10 mM) at 37°C for 1 h, respectively. After being washed three times by PBS, cells were further incubated solely with **BT-4** (10 μM, 1% DMSO, v%) for another 5 h at 37°C. All cells were then washed with PBS three times and subjected to a NIR-II fluorescence microscope (λ_{ex} = 808 nm, λ_{em} = 1000-1200 nm).

2.11 Detection of intracellular ROS generation

4T1 cells were seeded on confocal dishes (~5×10^4 cells/dish). After cells were incubated with **BT-4** (20 μM) for 6 h, the medium was replaced by DCFH-DA (20 μM) for further incubation (20 min). Then the medium was replaced with fresh medium, and cells were illuminated with 808 nm laser (1.0 W cm^{-2}) for 5 min and subsequently visualized by an invert fluorescence microscope (λ_{ex} = 488 nm; λ_{em} = 520-550 nm).

2.12 Apoptosis Analyses

4T1 cells were incubated with **BT-4** (20 μM) or serum-free medium for 24 h and then treated with or without 808 nm laser (1.0 W cm^{-2}, 5 min). After incubation for another 24 h, cells were stained with Annexin V-FITC and PI for 15 min and analyzed with flow cytometry. The data were analyzed with GraphPad Prism 8.0 statistical analysis software. All other measurements were analyzed by one-way ANOVA.

2.13 Cell Cycle Analyses

4T1 cells were incubated with BT-4 (10 μM) or serum-free medium for 24 h and then treated with or without 808 nm laser (1.0 W cm^{-2}, 5 min). After incubation for another 24 h, cells were then

lysed by RNaseA (100 μg/mL, 37°C) for 20 min. After that, cells were stained with PI (100 μg/mL, r.t.) for 15 min and subsequently analyzed cell cycle distribution by flow cytometry.

2.14 *In vivo* anti-tumor activity

Ethical approval for the animal experiments reported here was obtained from Central China Normal University. All animal experiments involved in this study were conducted in accordance with the Guide for the Care and Use of Laboratory Animals of Central China Normal University and use Committee (CCNU-IACUC-2023-001).

Tumor volume and body weight were measured for animals in all experiments. Tumor volume was determined by measuring the tumor in two dimensions with calipers and calculated using the formula tumor volume = (length × width^2)/2. The mice were divided into four groups randomly (n = 4) when the mean tumor volume reached about 60 mm^3 and this day was set as day 0. Mice were treated with control, control + laser, **BT-4** (at a dose of 1 mg Pt per kg body weight), **BT-4** + laser. Tumor volumes and body weights were measured every 2 days in the case of the 4T1 tumor-bearing mice. At 12 h post intratumoral injection, tumors in groups 2 and 4 were irradiated with an 808 nm laser (1.0 W cm^{-2}, 5 min) on day 0 and day 3, respectively. The tumor inhibition study was stopped on the 15th day for these 4T1 tumor-bearing mice and the tumors from all experimental groups were completely excised at the end of the treatment period. The data were analyzed with GraphPad Prism 8.0 statistical analysis software. All other measurements were analyzed by one-way ANOVA.

2.15 Histological examination

Upon completion of the treatment, the mice were sacrificed. The tumors and organs including heart, liver, spleen, lung, and kidney were resected, immersed in 4% paraformaldehyde and stored at 4°C for seven days. The sections of the tumors and organs were obtained as paraffin-embedded samples and stained with hematoxylin and eosin (H&E) and TdT-mediated dUTP Nick-End Labeling (TUNEL). Deep blue-purple hematoxylin and pink Eosin 18 stained nucleic acids and proteins, and TUNEL stained the DNA of apoptotic cells, respectively. A Carl Zeiss Axio Imager Z2 microscope was used to observe the tissue structure and cell state of the sections.

3. Synthetic Procedures and Characterization Data

3.1 Synthetic procedures and compound characterization

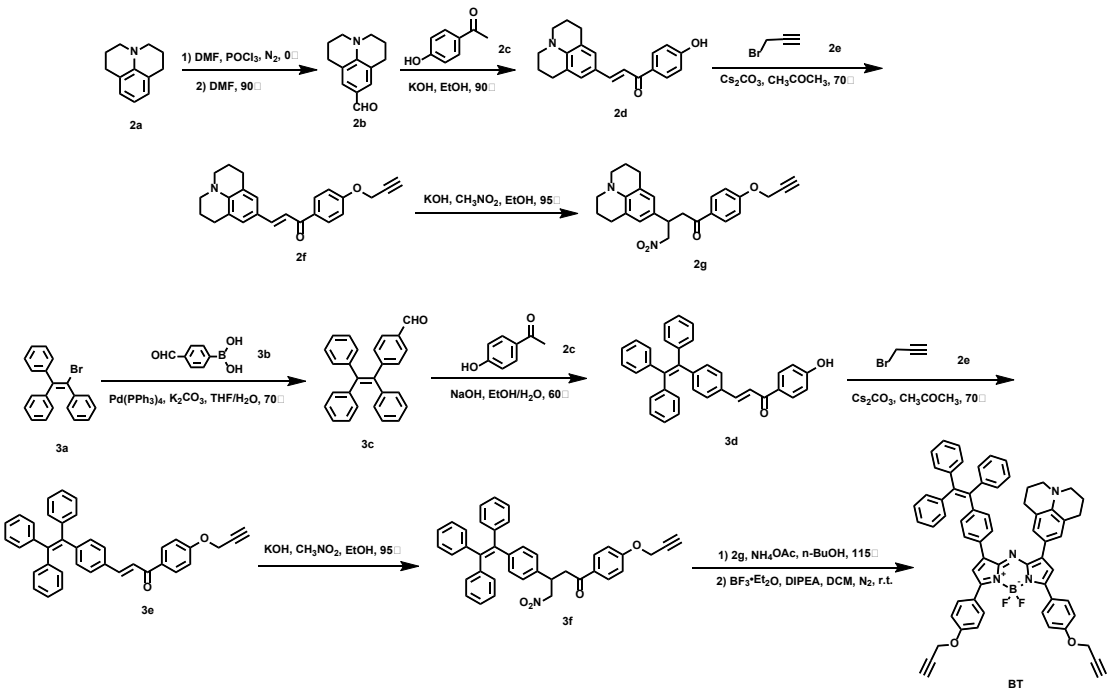

Scheme S1. Synthesis of **BT**.

Synthesis of compound 2b

DMF (2.3 mL) was added to freshly distilled $POCl_3$ (2 mL) under an atmosphere of N_2 at 0°C and the mixture was stirred for 1 h.[S2] After the dropwise addition of **2a** (2.50 g, 14.43 mmol) in DMF (10 mL), the mixture was stirred for 6 h at 90°C and then poured into ice water. After stirring for 2 h at room temperature, the mixture was extracted with ethyl acetate (EA), and the organic fractions were collected and dried over anhydrous Na_2SO_4. The crude product obtained in this way was purified by silica gel chromatography (petroleum ether (PE): EA = 20: 1, v: v) to afford a yellow solid **2b** (2.65 g, 91% yield). ^{1}H NMR (400 MHz, $CDCl_3$) δ: 9.62 (s, 1H), 7.31 (d, *J* = 8.0 Hz, 2H), 3.32 (t, *J* = 5.6 Hz, 4H), 2.80 (t, *J* = 6.0 Hz, 4H), 2.02 – 1.96 (m, 4H). ^{13}C NMR (100 MHz, $CDCl_3$) δ: 190.2, 147.9, 129.5, 124.0, 120.3, 50.1, 27.7, 21.3.

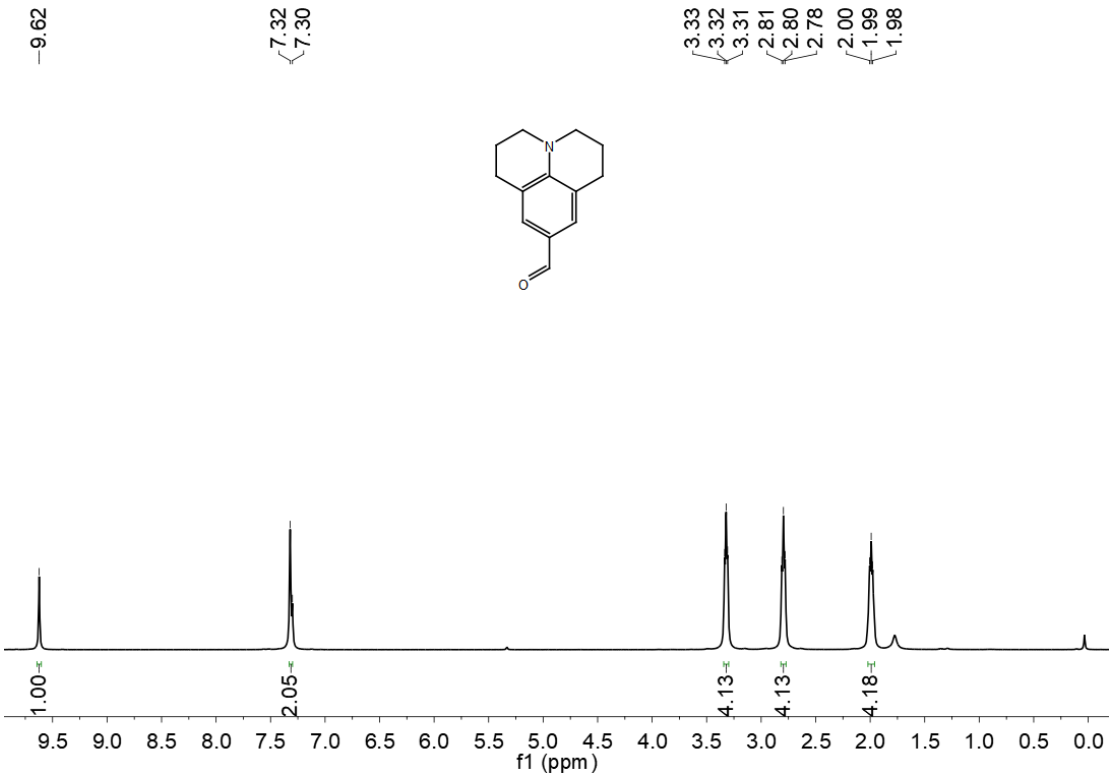

Figure S1. ^{1}H NMR spectrum (400 MHz, $CDCl_3$, 298 K) of **2b**.

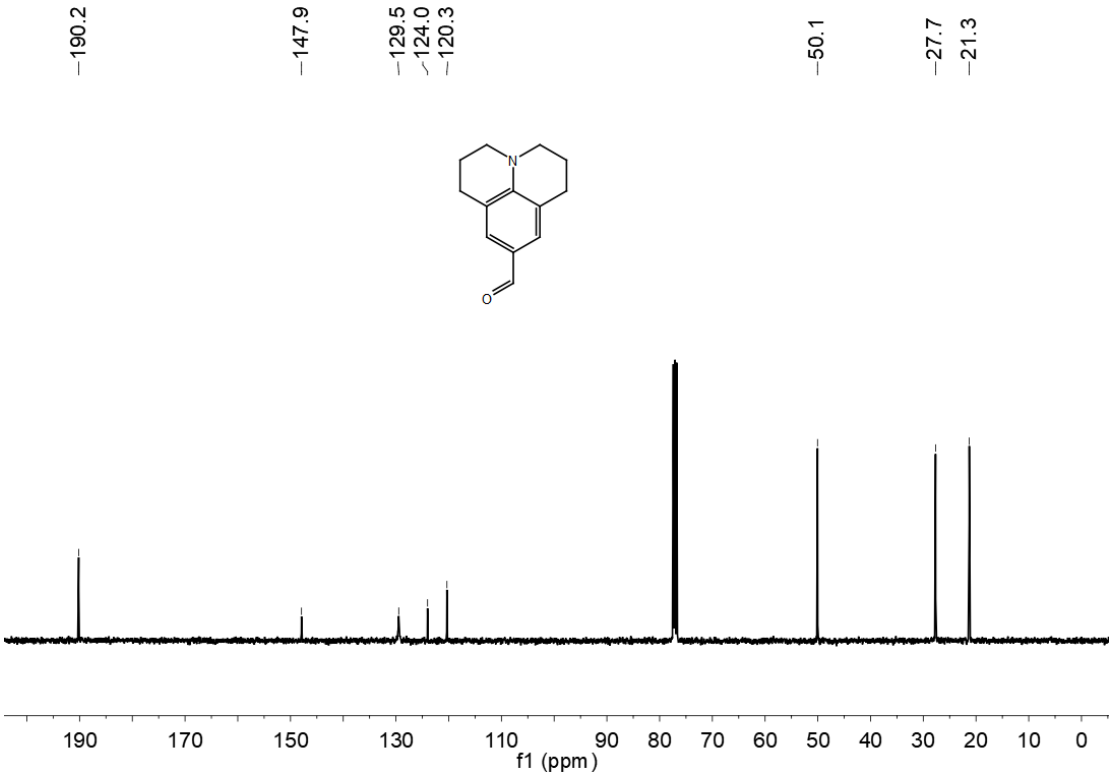

Figure S2. ^{13}C NMR spectrum (100 MHz, $CDCl_3$, 298 K) of **2b**.

Synthesis of compound 2d

Compound **2b** (2.65 g, 13.17 mmol) and compound **2c** (1.44 g, 10.53 mmol) were dissolved in ethanol (EtOH, 30 mL). Potassium hydroxide (3.69 g, 65.83 mmol) was then added and the reaction mixture was stirred at 90°C for 24 h. The EtOH and other volatiles were removed under reduced pressure and the resultant aqueous solution was diluted with brine and extracted with EA. The combined organic fractions were dried over anhydrous Na_2SO_4. The organic phase was subject to filteration before being concentrated under reduced pressure to afford a crude residue that was purified by a silica gel column (PE: EA = 20: 1, v: v) to afford **2d** as a red solid (2.38 g, 57% yield). ^{1}H NMR (400 MHz, $CDCl_3$) δ: 7.98 (d, *J* = 8.4 Hz, 2H), 7.71 (d, *J* = 15.6 Hz, 1H), 7.29 (s, 1H), 7.11 (s, 2H), 6.91 (d, *J* = 8.4 Hz, 2H), 3.25 (t, *J* = 5.6 Hz ,4H), 2.77 (t, *J* = 6.0 Hz, 4H), 2.00 – 1.95 (m, 4H). ^{13}C NMR (100 MHz, $CDCl_3$) δ: 189.4, 160.1, 146.1, 145.3, 130.9, 128.2, 121.7, 121.0, 115.4, 115.3, 50.0, 27.7, 21.6.

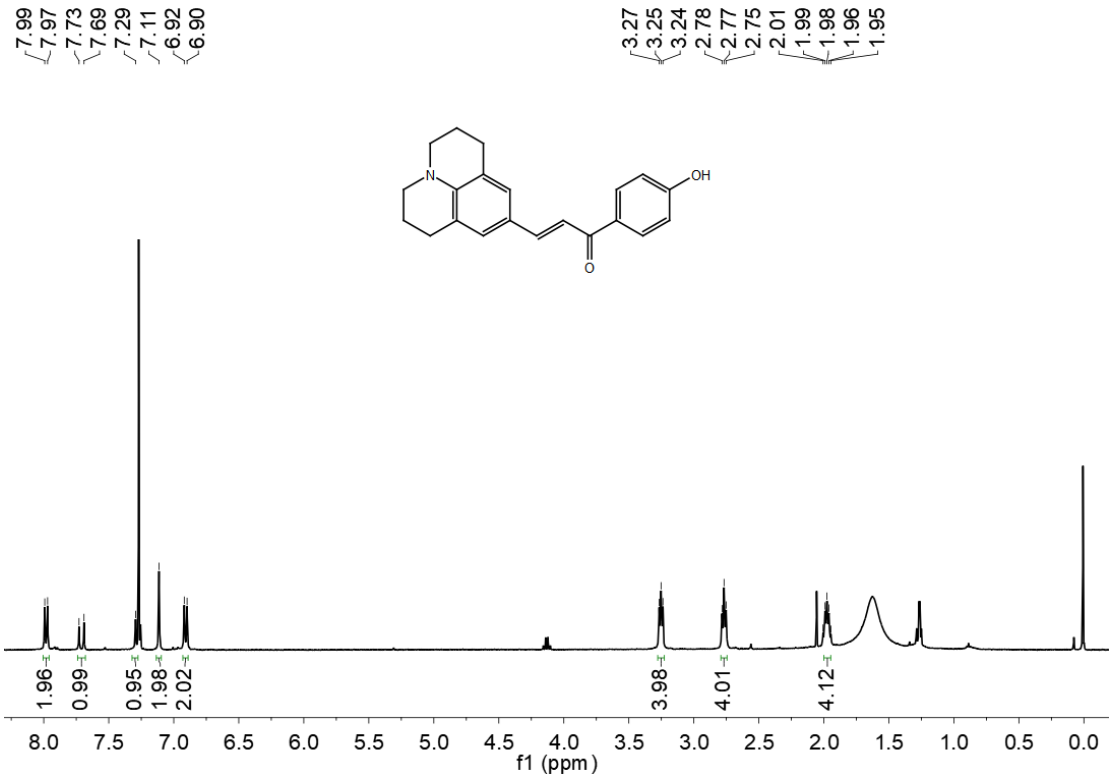

Figure S3. ^{1}H NMR spectrum (400 MHz, $CDCl_3$, 298 K) of **2d**.

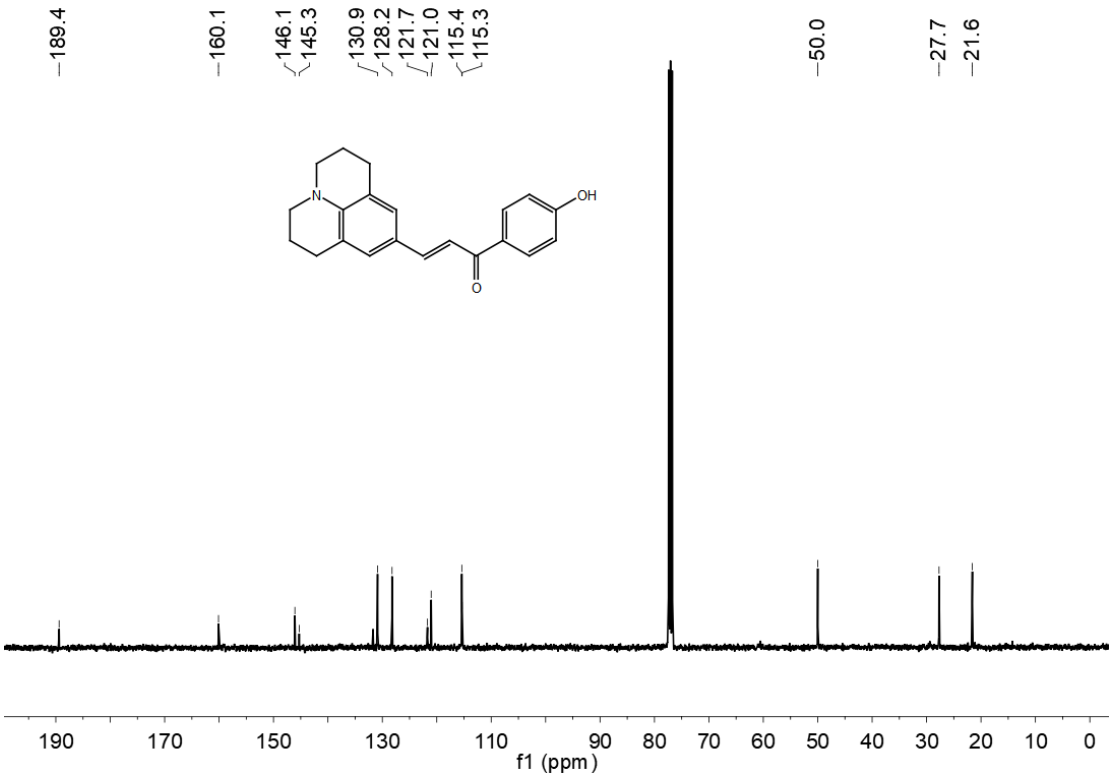

Figure S4. ^{13}C NMR spectrum (100 MHz, $CDCl_3$, 298 K) of **2d**.

Synthesis of compound 2f

Compound **2d** (2.38 g, 7.45 mmol) and cesium carbonate (Cs_2CO_3, 2.43 g, 7.45 mmol) were added to a round-bottom flask in an anhydrous and oxygen-free environment. **2e** (0.96 mL, 11.18 mmol) and acetone (25 mL) were injected into the reaction system and then refluxed at 70°C for 10 h. After the reaction was completed, the reaction liquid was distilled under vacuum and extracted with sodium bicarbonate aqueous solution and EA. The combined organic phase was dried with anhydrous Na_2SO_4, and the crude product was purified by silica gel column (PE: EA = 30:1, v: v) to obtain a red solid **2f** (1.75 g, 66% yield). ^1H NMR (400 MHz, $CDCl_3$) δ: 8.02 (d, *J* = 8.8 Hz, 2H), 7.70 (d, *J* = 15.6 Hz, 1H), 7.25 (d, *J* = 2.0 Hz, 1H), 7.11 (s, 2H), 7.04 (d, *J* = 8.8 Hz, 2H), 4.76 (d, *J* = 2.4 Hz, 2H), 3.24 (t, *J* = 5.6 Hz, 4H), 2.76 (t, *J* = 6.4 Hz, 4H), 2.57 – 2.54 (m, 1H), 2.00 – 1.93 (m, 4H). ^{13}C NMR (100 MHz, $CDCl_3$) δ: 188.9, 160.6, 145.8, 145.2, 132.9, 130.4, 128.1, 121.7, 121.0, 115.4, 114.5, 78.0, 76.0, 55.9, 50.0, 27.7, 21.6.

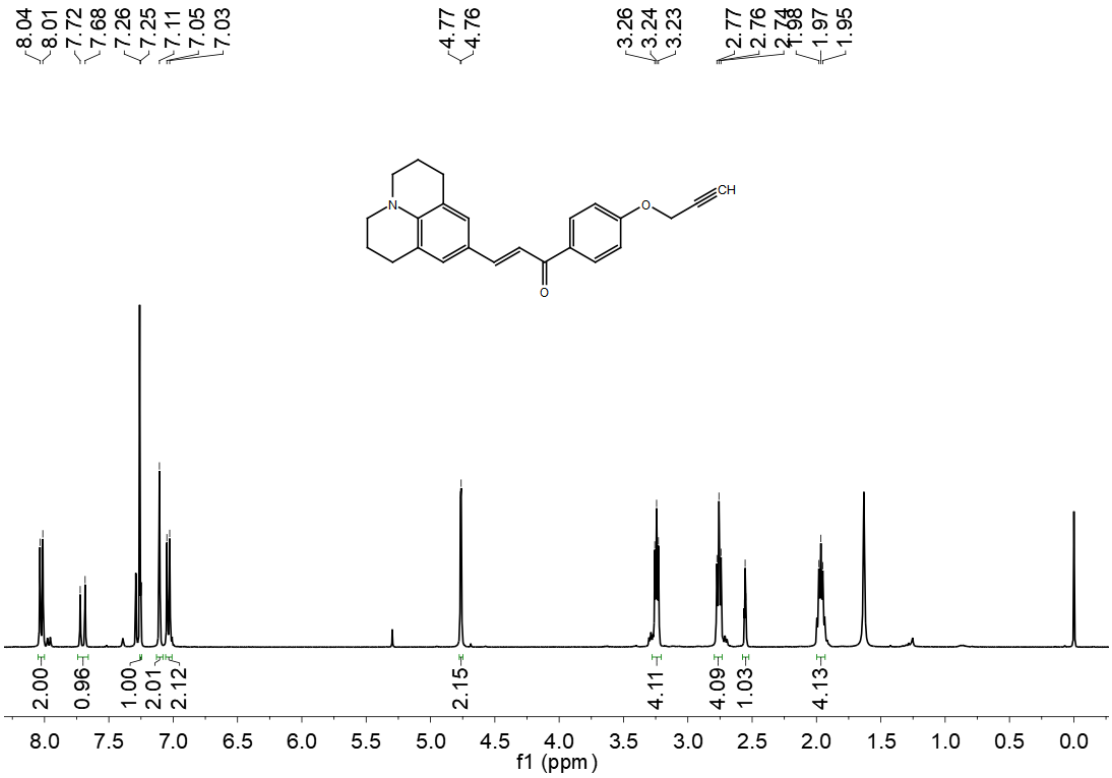

Figure S5. ^{1}H NMR spectrum (400 MHz, $CDCl_3$, 298 K) of **2f**.

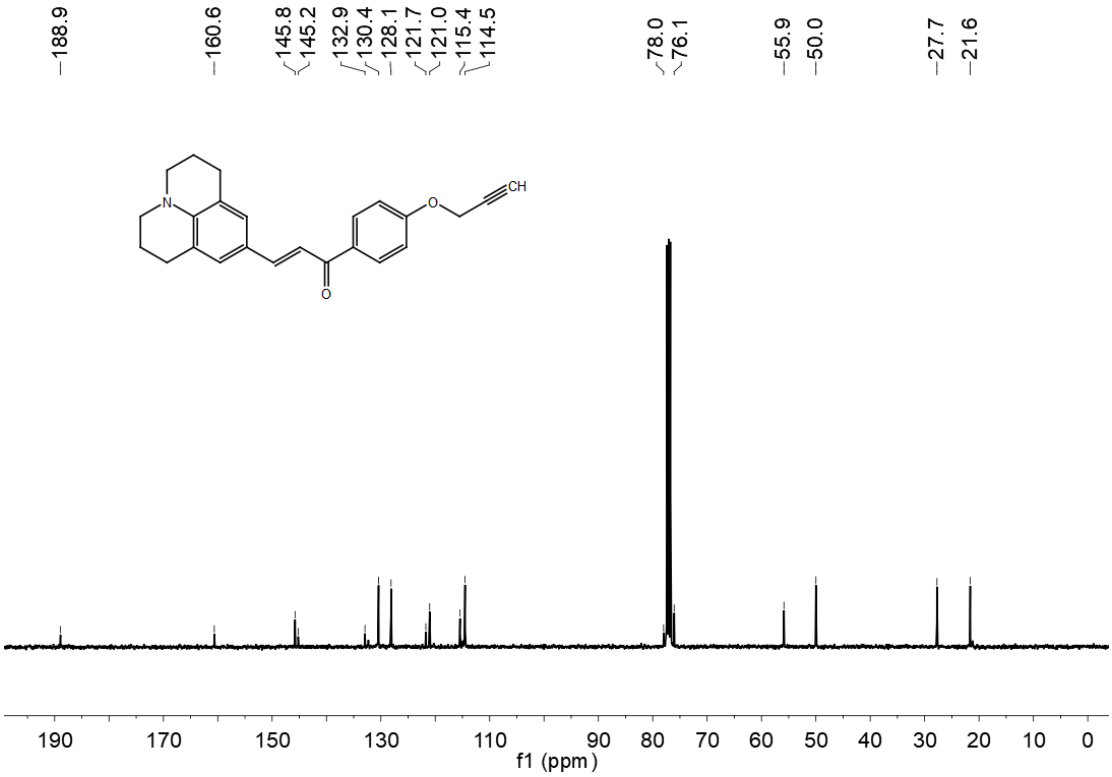

Figure S6. ^{13}C NMR spectrum (100 MHz, $CDCl_3$, 298 K) of **2f**.

Synthesis of compound 2g

The compound **2f** (1.75 g, 4.90 mmol) and potassium hydroxide (KOH, 0.41 g, 7.34 mmol) were added to a round-bottomed flask, followed by EtOH (25 mL) and nitromethane (CH_3NO_2, 3.93 mL, 73.44 mmol) respectively. The mixture was refluxed at 95°C for 15 h. After the reaction was completed and the reaction solvent was removed by vacuum distillation, and the residue was extracted with ethyl acetate and saturated salt water. The crude product was purified by silica gel column (PE: EA = 20:1, v: v) to obtain an orange-red oil product **2g** (1.14 g, 56% yield). ^{1}H NMR (400 MHz, $CDCl_3$) δ: 7.92 (d, *J* = 8.8 Hz, 2H), 7.00 (d, *J* = 8.8 Hz, 2H), 6.64 (s, 2H), 4.75 (d, *J* = 2.0 Hz, 2H), 4.72 (t, *J* = 5.2 Hz, 1H), 4.58 (dd, *J* = 12.4, 8.0 Hz, 1H), 4.03 – 3.93 (m, 1H), 3.32 (dd, *J* = 10.0, 6.0 Hz, 2H), 3.09 (t, 5.6 Hz, 4H), 2.70 (t, *J* = 6.4 Hz, 4H), 2.55 (t, *J* = 2.4 Hz, 1H), 1.97 – 1.91 (m, 4H). ^{13}C NMR (100 MHz, $CDCl_3$) δ: 196.0, 161.5, 142.4, 130.4, 130.3, 125.8, 121.8, 114.7, 80.0, 77.7, 76.3, 55.9, 49.9, 41.7, 38.7, 27.7, 22.0.

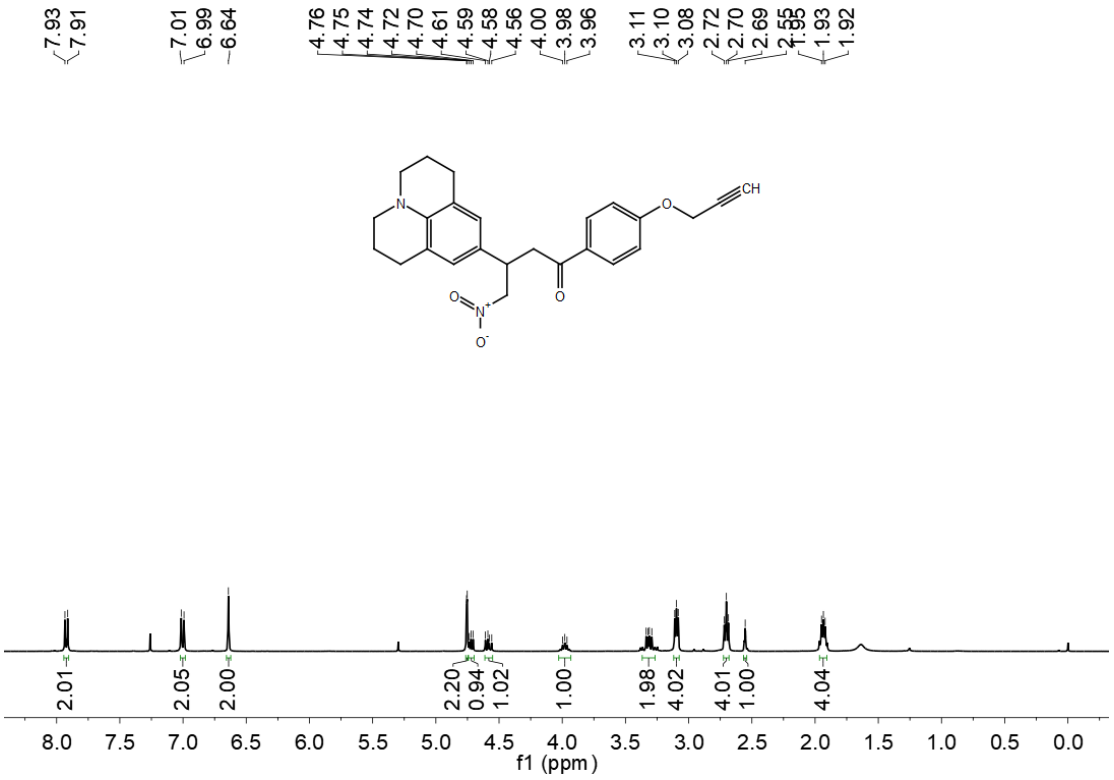

Figure S7. ^{1}H NMR spectrum (400 MHz, $CDCl_3$, 298 K) of **2g**.

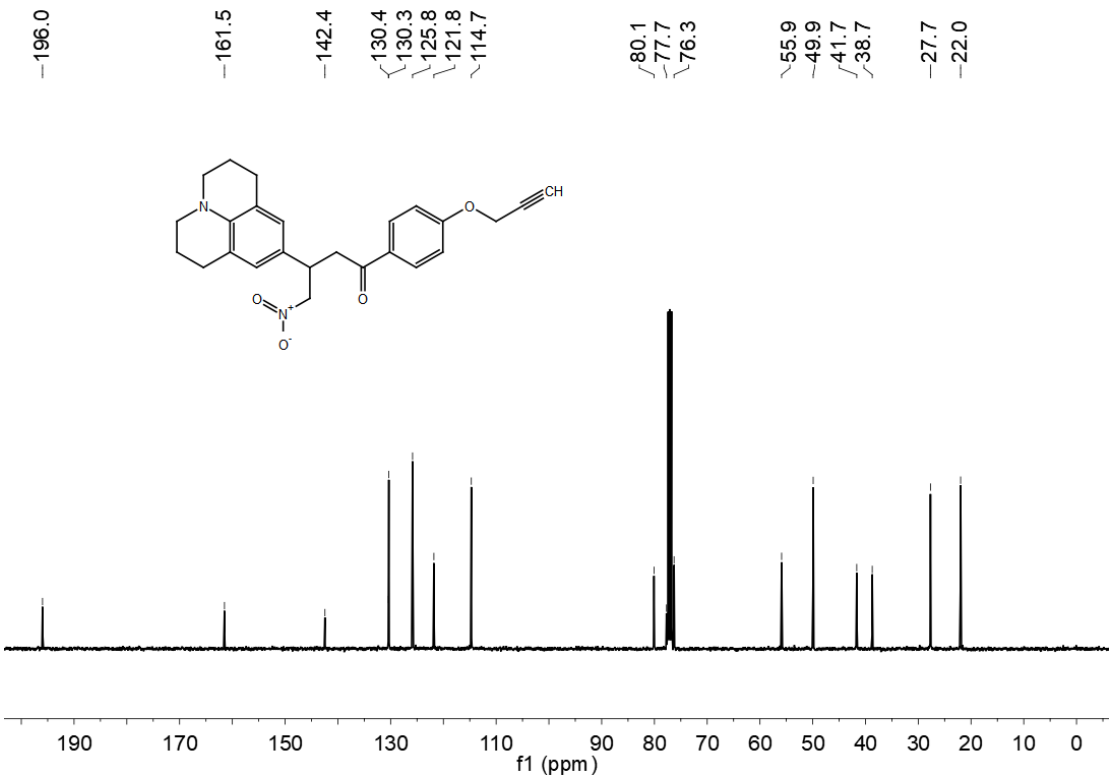

Figure S8. ^{13}C NMR spectrum (100 MHz, $CDCl_3$, 298 K) of **2g**.

Synthesis of compound 3c

The compounds **3a** (5.00 g, 14.91 mmol), **3b** (2.46 g, 16.41 mmol) and tetrakis(triphenylphosphine)palladium ($Pd(PPh_3)_4$, 0.18 g, 0.15 mmol), were added to a round bottom flask. Under nitrogen atmosphere, tetrahydrofuran (THF, 40 mL) and potassium carbonate aqueous solution (4 M, 10 mL) were injected and the mixture was stirred at 70°C for 18 h. After the reaction is completed, it is cooled to room temperature and the reaction liquid is distilled under vacuum. The residue was extracted with ethyl acetate and water, combined with organic phase and dried with anhydrous sodium sulfate. The crude product was purified by silica gel column (PE: EA = 50:1, v: v) to afford a light yellow solid **3c** (4.58 g, 85% yield). ^1H NMR (400 MHz, $CDCl_3$) δ: 9.94 (s, 1H), 7.65 (d, *J* = 7.2 Hz, 2H), 7.23 (d, *J* = 7.2 Hz, 2H), 7.18 – 7.13 (m, 9H), 7.09 – 7.03 (m, 6H). ^{13}C NMR (100 MHz, $CDCl_3$) δ: 192.0, 150.6, 143.1, 142.9, 139.8, 134.3, 132.0, 131.3, 131.3, 129.2, 128.0, 127.8, 127.1, 126.9, 126.9.

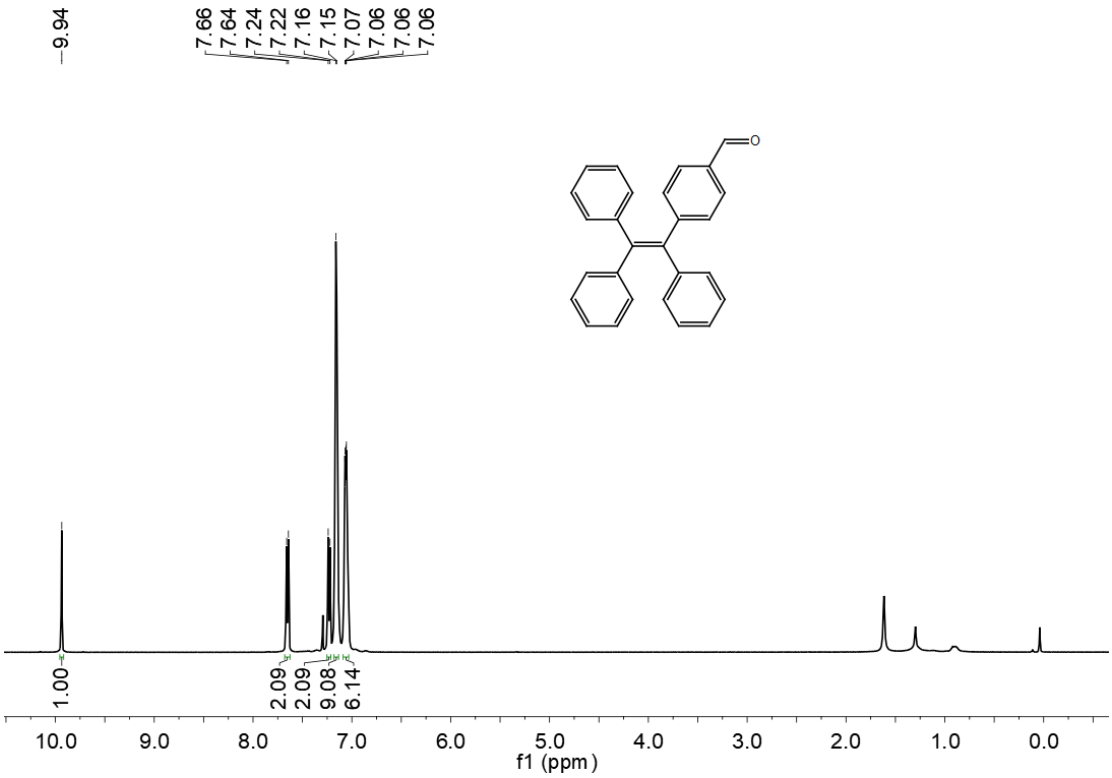

Figure S9. ^{1}H NMR spectrum (400 MHz, $CDCl_3$, 298 K) of **3c**.

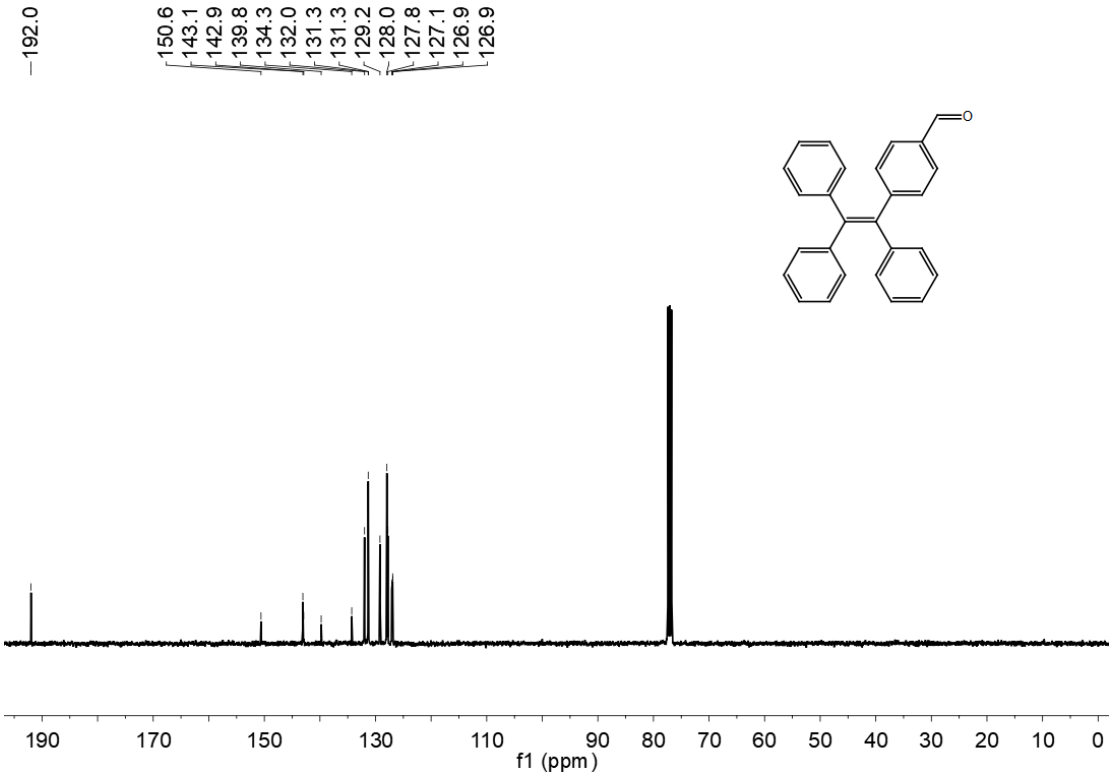

Figure S10. ^{13}C NMR spectrum (100 MHz, $CDCl_3$, 298 K) of **3c**.

Synthesis of compound 3d

The compound **3c** (4.58 g, 12.70 mmol) and compound **2c** (1.73 g, 12.70 mmol) were added into a 100 ml round-bottomed flask. And then sodium hydroxide aqueous solution (5 M, 10 mL) and anhydrous EtOH (50 mL) were added and the mixture was stirred at 60°C for 24 h. After the reaction was completed, the reaction liquid was distilled under reduced pressure and extracted with EA and saturated NH_4Cl solution. Then the organic phase was collected and dried with anhydrous Na_2SO_4. The crude product was purified by silica gel column (PE: EA = 20:1, v: v), to obtain an orange solid product **3d** (3.35 g, 55%). ^{1}H NMR (400 MHz, $CDCl_3$) δ: 8.00 (d, *J* = 8.8 Hz, 2H), 7.74 (d, *J* = 15.6 Hz, 1H), 7.48 (d, *J* = 15.6 Hz, 1H), 7.41 (d, *J* = 8.0 Hz, 2H), 7.17 – 7.13 (m, 9H), 7.11 – 7.03 (m, 9H), 6.98 – 6.95 (m, 2H). ^{13}C NMR (100 MHz, $CDCl_3$) δ: 189.9, 161.2, 146.6, 144.6, 143.4, 143.3, 142.1, 140.1, 132.8, 132.0, 131.4, 130.4, 128.0, 127.9, 127.9, 127.7, 126.8, 126.7, 121.3, 116.0.

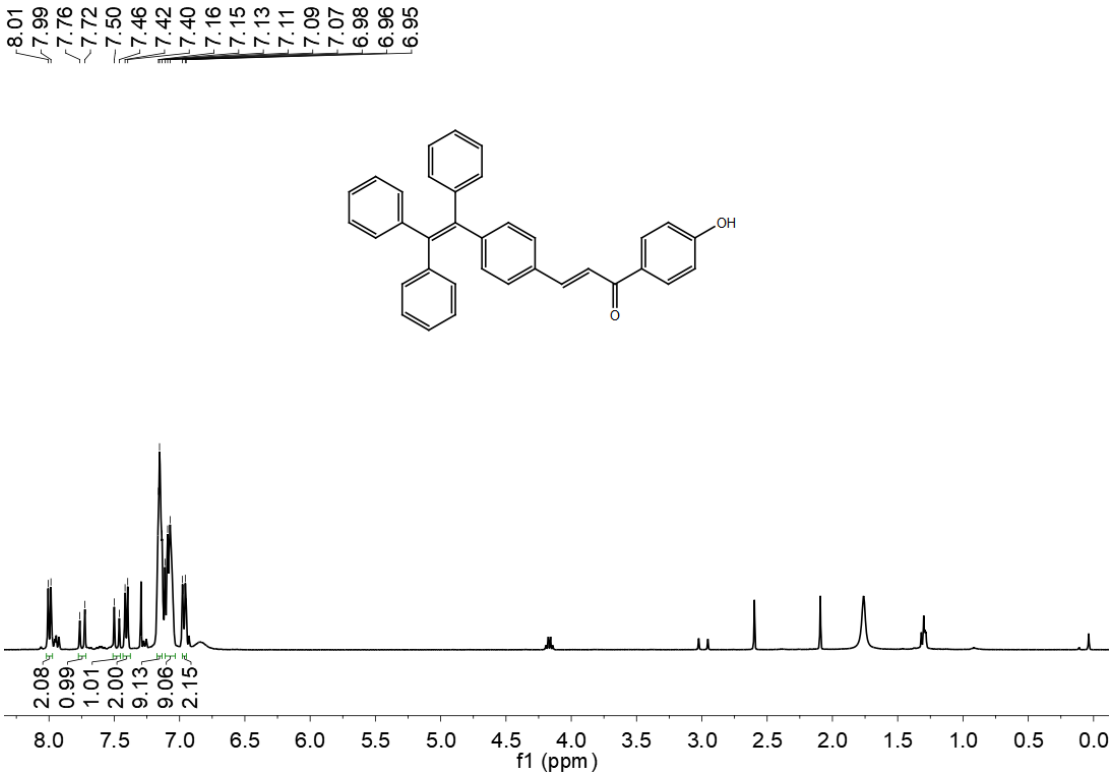

Figure S11. ^{1}H NMR spectrum (400 MHz, $CDCl_3$, 298 K) of **3d**.

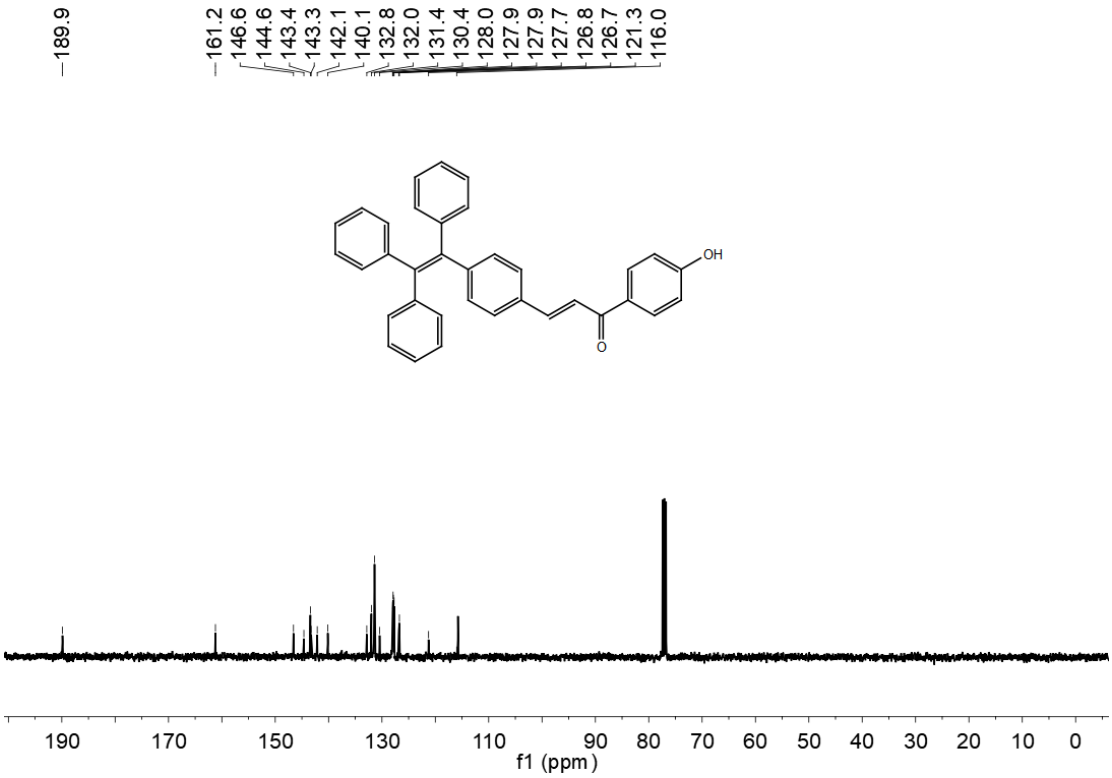

Figure S12. ^{13}C NMR spectrum (100 MHz, $CDCl_3$, 298 K) of **3d**.

Synthesis of compound 3e

The procedure was similar to that for complex **2f** except that **3d** (3.35 g, 7.00 mmol) was used instead of **2d**. The product was obtained as a yellow solid **3e** (1.95 g, 54% yield). ^1H NMR (400 MHz, $CDCl_3$) δ: 8.02 (d, *J* = 8.8 Hz, 2H), 7.71 (d, *J* = 15.6 Hz, 1H), 7.44 (d, *J* = 15.6 Hz, 1H), 7.38 (d, *J* = 8.4 Hz, 2H), 7.14 – 7.10 (m, 9H), 7.08 – 7.01 (m, 10H), 4.77 (d, *J* = 2.4 Hz, 2H), 2.56 (t, *J* = 2.4 Hz, 1H). ^{13}C NMR (100 MHz, $CDCl_3$) δ: 188.7, 161.2, 146.4, 144.0, 143.4, 143.3, 142.1, 140.2, 133.0, 132.0, 131.4, 131.4, 131.3, 130.7, 127.9, 127.9, 127.7, 126.8, 126.7, 121.3, 114.7, 77.8, 76.2, 55.9.

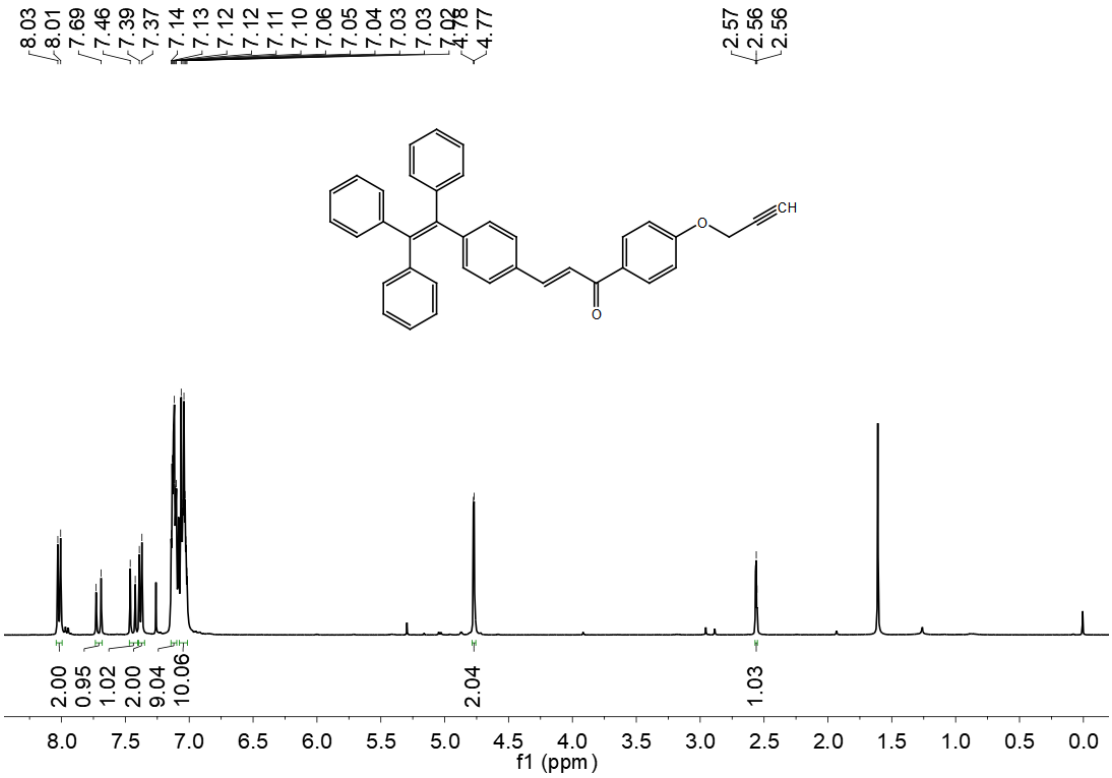

Figure S13. ^{1}H NMR spectrum (400 MHz, $CDCl_3$, 298 K) of **3e**.

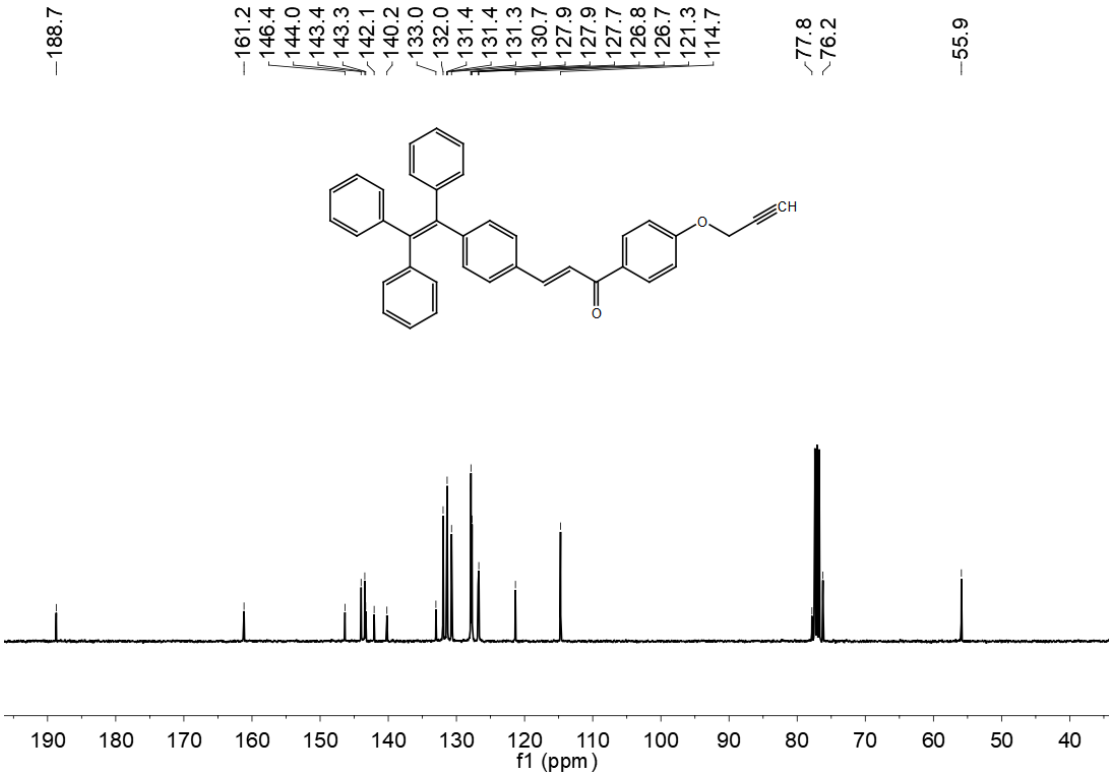

Figure S14. ^{13}C NMR spectrum (100 MHz, $CDCl_3$, 298 K) of **3e**.

Synthesis of compound 3f

The procedure was similar to that for complex **2g** except that **3e** (1.95 g, 3.77 mmol) was used instead of **2f**. The product was obtained as a yellow solid **3f** (0.89 g, 41% yield). ^{1}H NMR (400 MHz, $CDCl_3$) δ: 7.98 (d, *J* = 8.0 Hz, 2H), 7.19 – 7.14 (m, 9H), 7.11 – 7.06 (m, 10H), 7.04 (d, *J* = 6.8 Hz, 2H), 4.85 (s, 3H), 4.68 (t, *J* = 8.0 Hz, 1H), 4.26 – 4.13 (m, 1H), 3.41 (d, *J* = 6.5 Hz, 2H), 2.64 (s, 1H). ^{13}C NMR (100 MHz, $CDCl_3$) δ: 195.5, 161.6, 143.6, 143.4, 143.4, 143.4, 141.4, 140.2, 137.2, 131.9, 131.3, 130.3, 127.7, 127.7, 126.8, 126.6, 126.5, 114.8, 79.7, 77.7, 76.4, 55.9, 41.1, 39.2.

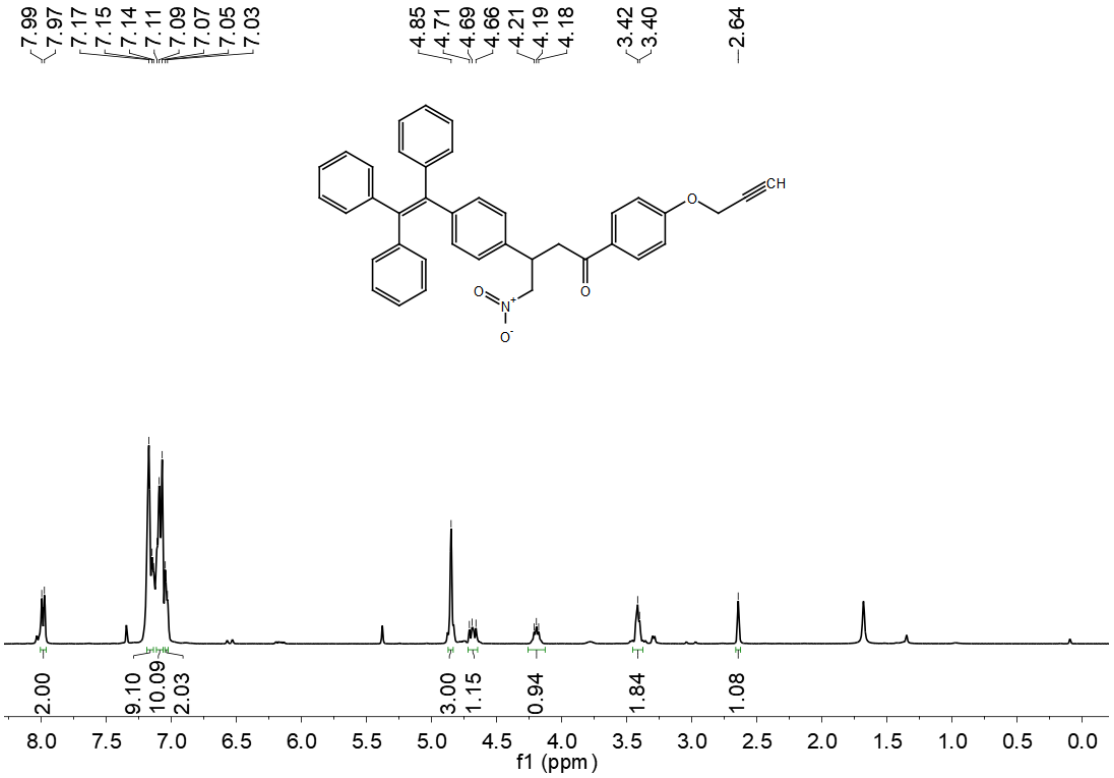

Figure S15. ^{1}H NMR spectrum (400 MHz, $CDCl_3$, 298 K) of **3f**.

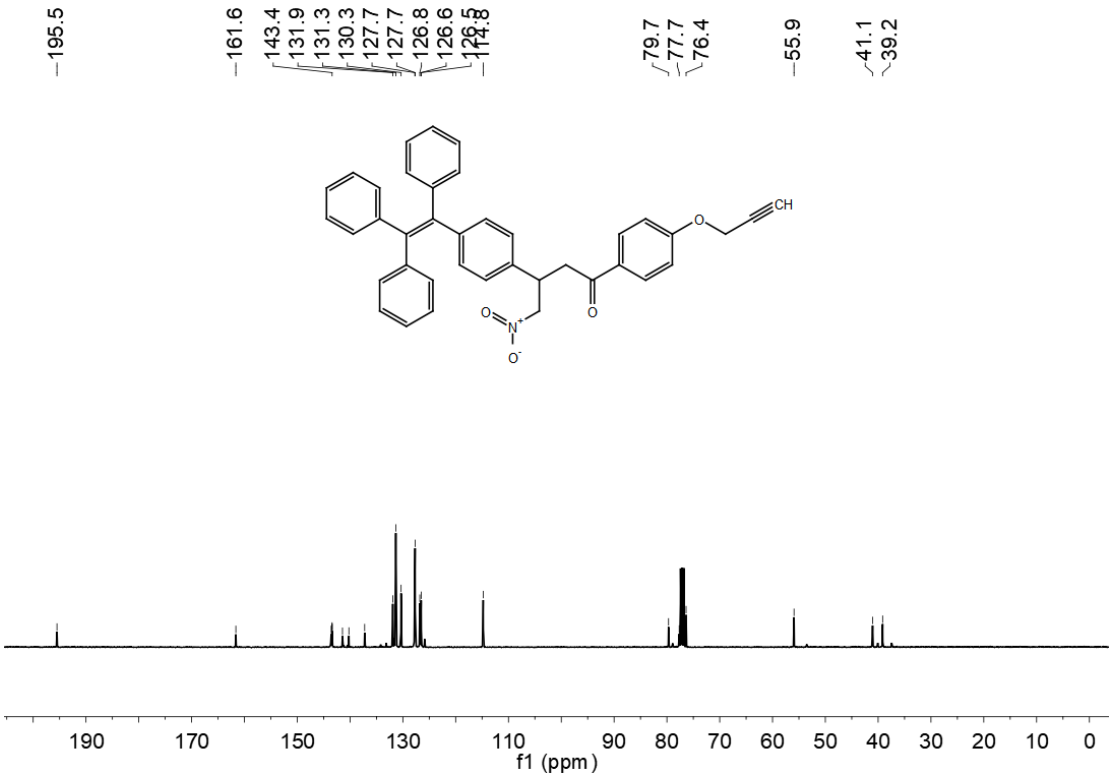

Figure S16. ^{13}C NMR spectrum (100 MHz, $CDCl_3$, 298 K) of **3f**.

Synthesis of compound BT

Compound **3f** (0.89 g, 1.54 mmol) and **2g** (0.64 g, 1.54 mmol) were dissolved in 1-butanol (20 mL). Ammonium acetate (NH_4OAc, 3.15 g, 40.86 mmol) was added and the reaction was stirred at 115°C for 12 h. The reaction was cooled to room temperature and the volume was taken to 5 mL under reduced pressure. The reaction mass was then filtered. The isolated solid was washed with ethanol (3 × 5 mL) to afford a dark blue film. The film (0.49 g, 0.66 mmol) was dissolved in anhydrous dichloromethane (DCM, 15 mL) and treated with anhydrous N,N-diisopropylethylamine (DIPEA, 1.14 mL, 6.55 mmol) and boron trifluoride etherate (BF_3•Et_2O, 1.24 mL, 9.83 mmol) and then stirred at room temperature under N_2 for 24 h. The resulting solution was diluted with water (20 mL) and extracted with DCM. The combined organic fractions were dried over anhydrous Na_2SO_4, filtered and concentrated under reduced pressure to afford a crude residue, which was purified via flash chromatography on a silica gel column (PE: DCM=1: 1, v: v) to afford **BT** as a blue solid (0.27 g, 52% yield). ^1H NMR (400 MHz, $CDCl_3$) δ: 8.05 (d, *J* = 8.8 Hz, 2H), 7.97 (d, *J* = 8.8 Hz, 2H), 7.88 (d, *J* = 8.0 Hz, 2H), 7.67 (s, 2H), 7.15 – 7.08 (m, 15H), 7.04 (dd, *J* = 8.4, 4.4 Hz, 6H), 6.85 (s, 1H), 6.75 (s, 1H), 4.74 (t, *J* = 2.4 Hz, 4H), 3.25 (t, *J* = 5.6 Hz, 4H), 2.63 (t, *J* = 6.0 Hz, 4H), 2.55 (d, *J* = 1.2 Hz, 2H), 1.90 – 1.84 (m, 4H). ^{13}C NMR (100 MHz, $CDCl_3$) δ: 159.6, 158.8, 153.4, 145.0, 143.8, 143.6, 141.5, 140.7, 131.6, 131.5, 131.4, 131.4, 130.9, 128.9, 128.3, 127.9, 127.7, 127.7, 126.7, 126.5, 126.0, 125.4, 121.4, 119.6, 116.7, 114.8, 114.8, 114.2, 78.3, 78.1, 76.0, 75.9, 55.9, 50.1, 27.8, 21.6.

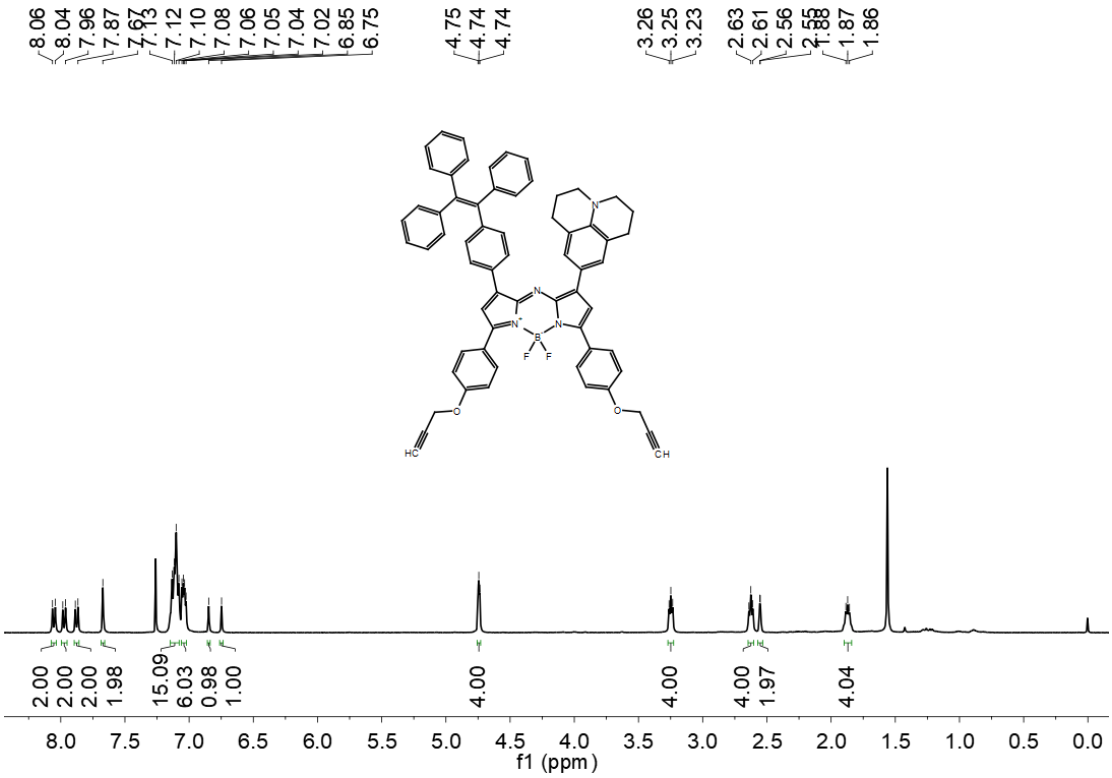

Figure S17. ^{1}H NMR spectrum (400 MHz, $CDCl_3$, 298 K) of **BT**.

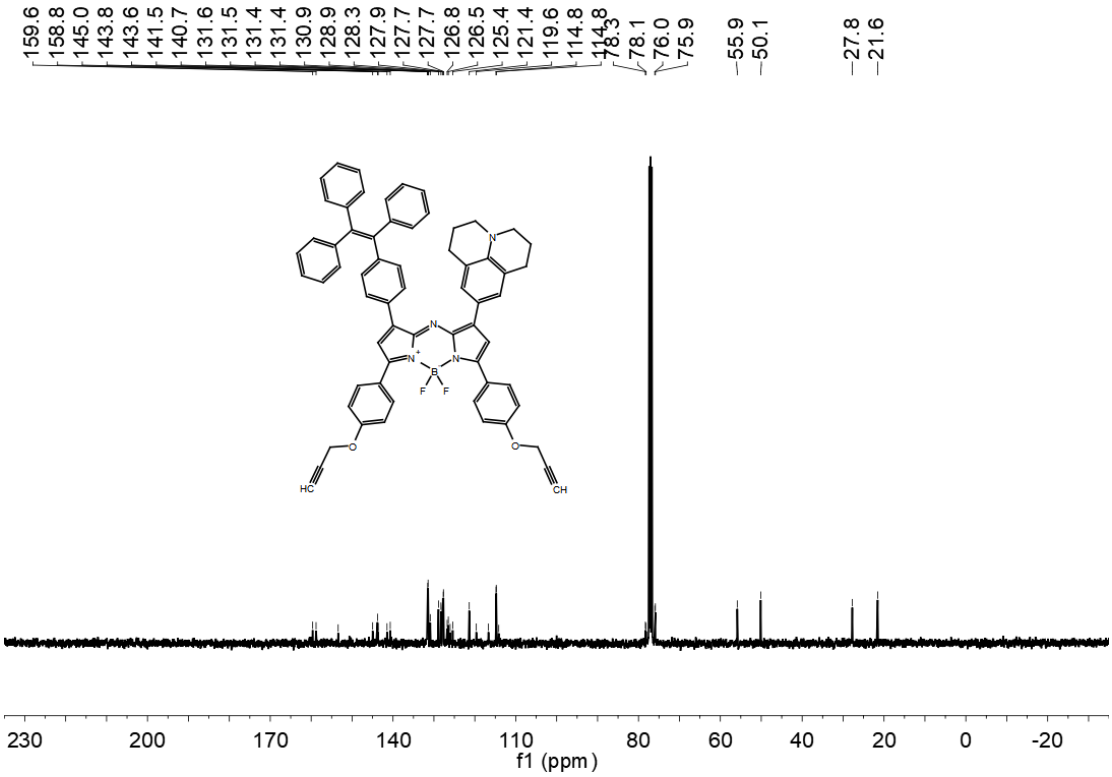

Figure S18. ^{13}C NMR spectrum (100 MHz, $CDCl_3$, 298 K) of **BT**.

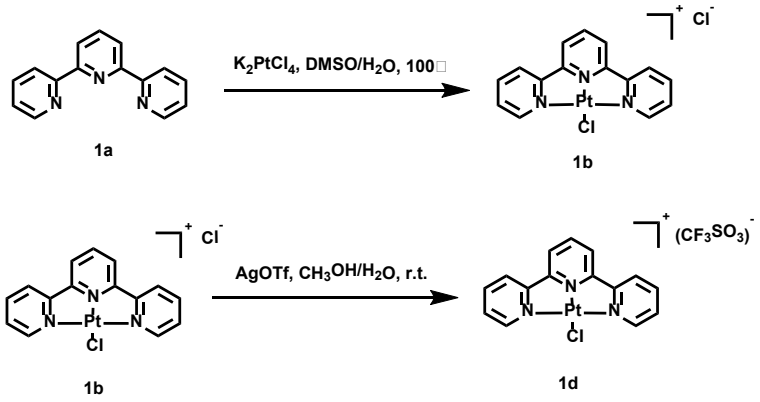

Scheme S2. Synthesis of Pt units.

Synthesis of compound 1b

Compound **1a** (300 mg, 1.28 mmol) was placed in a round-bottom flask and 5 mL of dimethyl sulfoxide was added. Subsequently, potassium tetrachloroplatinate(II) (K_2PtCl_4, 534 mg, 1.28 mmol) was dissolved water in (5 mL) and dropped into the mixture. After reacting at 100°C overnight and then cooling to room temperature, hydrochloric acid was slowly added, and an orange-red solid was precipitated and then filtrated. The isolated solid was washed with methanol and the product was obtained as orange-red solid **1b** (603 mg, 94% yield). ^{1}H NMR (400 MHz, D_2O) δ: 8.13 – 8.04 (m, 3H), 7.86 (d, *J* = 8.2 Hz, 6H), 7.37 (t, *J* = 6.6 Hz, 2H). MS (ESI-MS) m/z: calculated for [**1b** – Cl]$^+$: 463.80855, found 464.02765.

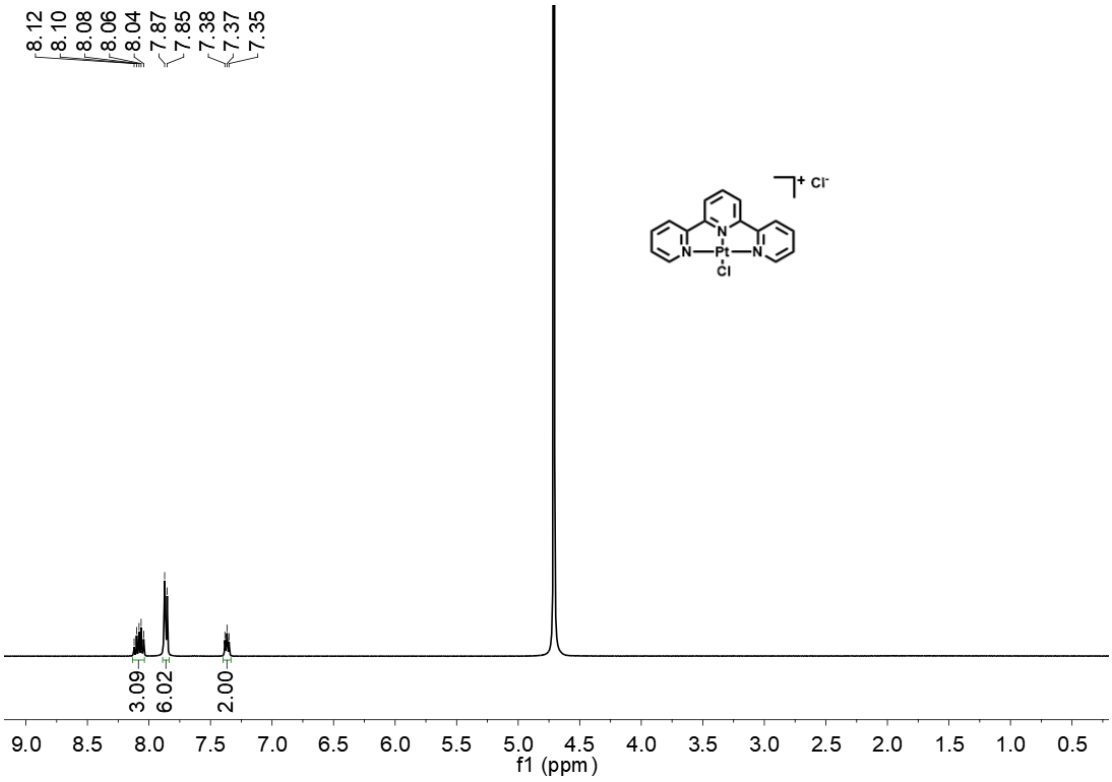

Figure S19. ^{1}H NMR spectrum (400 MHz, D_2O, 298 K) of **1b**.

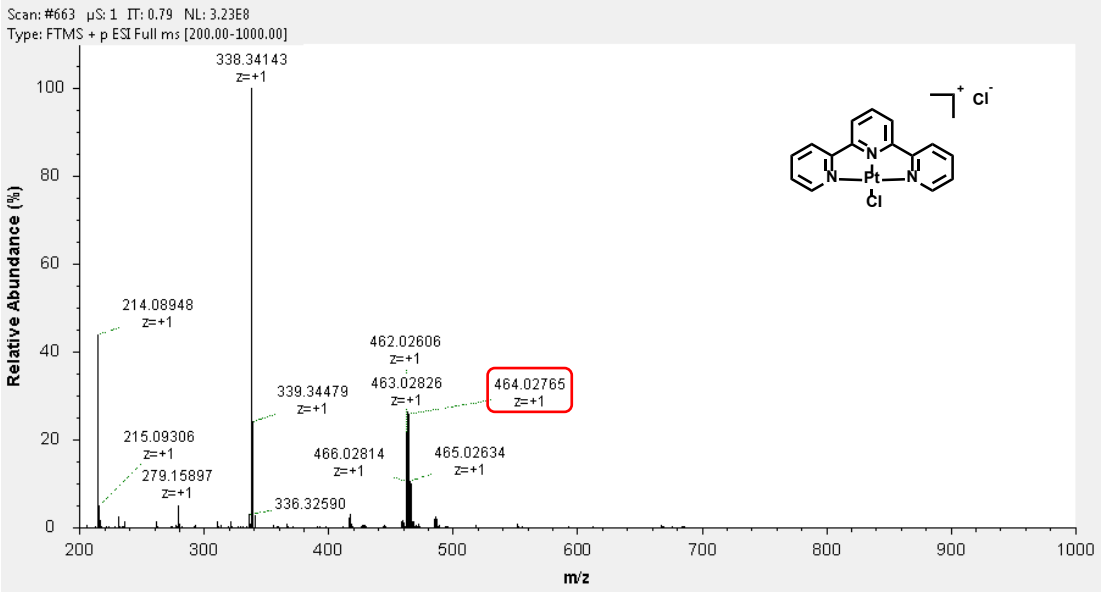

Figure S20. ESI-MS spectrum of **1b**.

Synthesis of compound 1d

Compound **1b** (100 mg, 0.20 mmol) was dissolved with water (8 mL) and stir evenly. Silver trifluoromethyl sulfonate (62 mg, 0.24 mmol) was dissolved in methanol (2 mL) and dropped into the aqueous solution. After stirring at room temperature for 12 hours, a large amount of sediment precipitated. After filtrating and washing with water. The product was obtained as orange-yellow solid **1d** (115 mg, 94% yield). ^{1}H NMR (400 MHz, DMSO) δ: 8.85 (d, *J* = 4.8 Hz, 2H), 8.62 (s, 5H), 8.53 – 8.49 (m, 2H), 7.95 – 7.92 (m, 2H).^{19}F NMR (400 MHz, DMSO) δ: -77.8 (s).

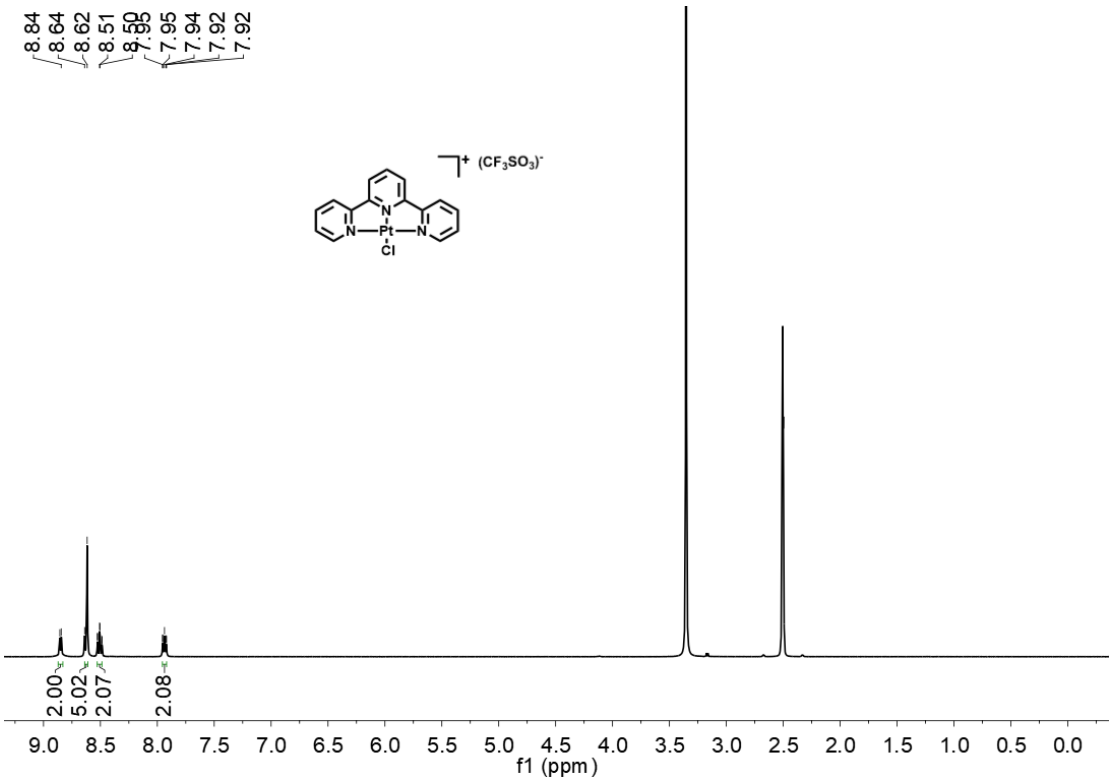

Figure S21. ^{1}H NMR spectrum (400 MHz, DMSO-d_6 , 298 K) of **1d**.

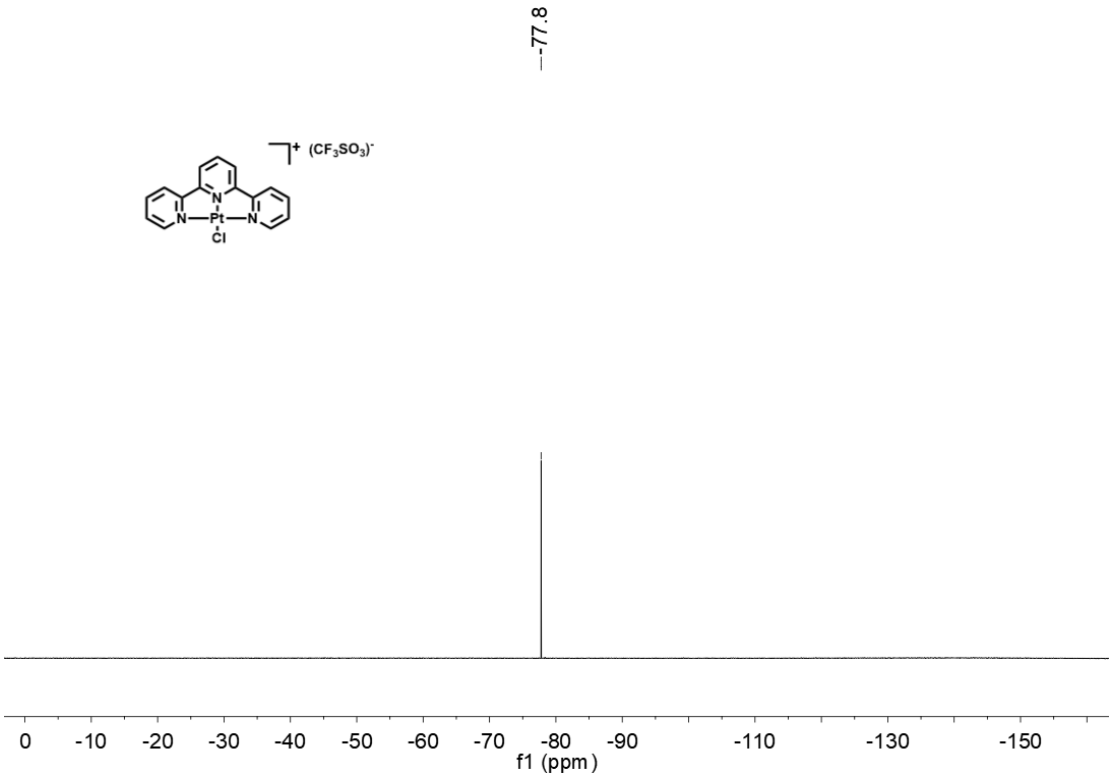

Figure S22. ^{19}F NMR spectrum (400 MHz, DMSO-d_6, 298 K) of **1d**.

Synthesis of compound BT-4

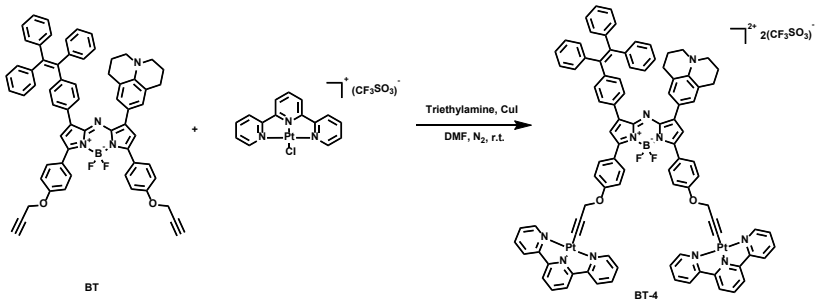

Compound **BT** (20 mg, 0.02 mmol) and compound **1d** (25 mg, 0.04 mmol) were added to two-necked flasks. Anhydrous DMF (15 mL), cuprous iodide (1.5 mg, 7.54 μmol), and triethylamine (35 μL, 0.25 mmol) were added successively under nitrogen conditions. After stirring at room temperature for 12 hours, the reaction liquid was distilled under reduced pressure. Recrystallization operations were carried out three times using DMF and ether to obtain the deep-green solid **BT-4** (29 mg, 66% yield). ^{1}H NMR (400 MHz, DMSO-d_6) δ: 8.90 (d, J = 12.0 Hz, 2H), 8.84 – 8.69 (m, 2H), 8.62 (s, 4H), 8.50 (d, J = 3.2 Hz, 2H), 8.46 – 8.37 (m, 2H), 8.36 – 8.01 (m, 10H), 7.95 (s, 4H), 7.88 – 7.34 (m, 10H), 7.32 – 6.92 (m, 16H), 6.67 (s, 2H), 4.95 (s, 4H), 2.88 (t, J = 12.2 Hz, 4H), 2.72 (s, 4H), 1.99 (d, J = 12.0 Hz, 4H). MS (ESI-TOF-MS) m/z: calculated for [**BT-4** – 2$(CF_3SO_3)^-$]$^{2+}$: 904.2481, found 904.1833.

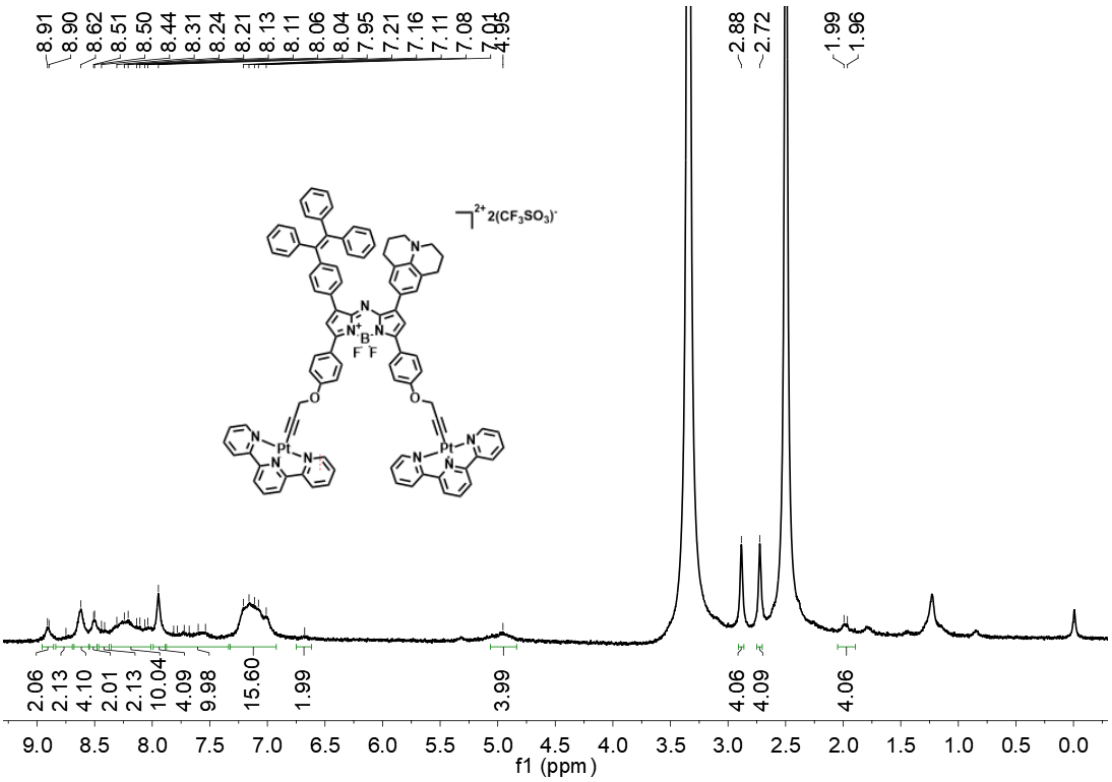

Figure S23. ^{1}H NMR spectrum (400 MHz, DMSO-d_6, 298 K) of **BT-4**.

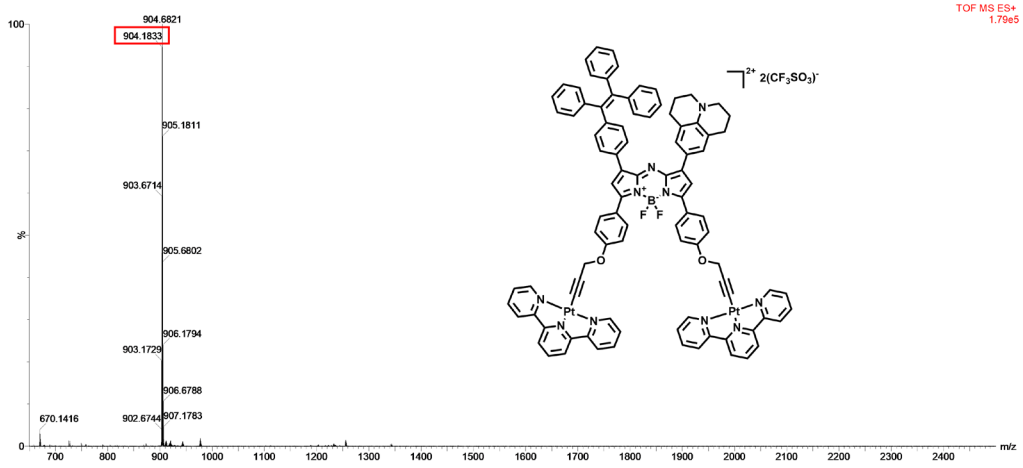

Figure S24. ESI-TOF-MS spectrum of **BT-4**.

3.2 Supplementary Figures

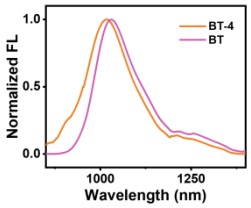

Figure S25. Normalized fluorescence emission of BT and BT-4 (10 μM) in DMF.

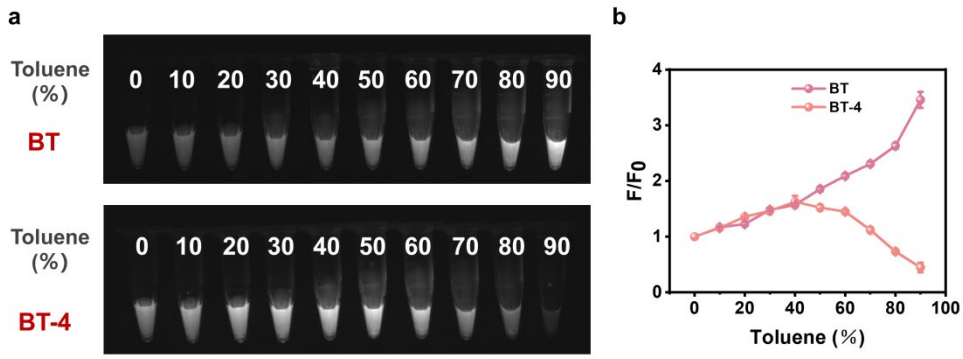

Figure S26. Fluorescence images (a) and relevant plots (b) of BT and BT-4 (10 μM) in DMSO/toluene mixture of different volume ratios with LP1000 filters (excited at 808 nm; exposure time: BT, 7 ms; BT-4, 50 ms).

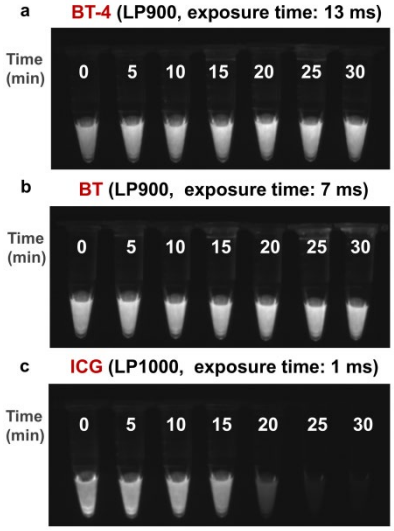

Figure S27. Fluorescence images of **BT-4** (a), **BT** (b) and ICG (c) in DMSO (50 μM) with different filters and exposure time after irradiation by 808 nm laser (1.0 W·cm^{-2}) for 0-30 min.

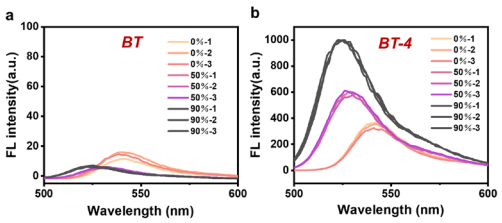

Figure S28. ROS generation of **BT** and **BT-4** (5 μM) in DMSO/H_2O mixture of different volume ratios illuminated by 808 nm laser (1.0 W cm^{-2}, 30 s) using DCFH-DA as an indicator.

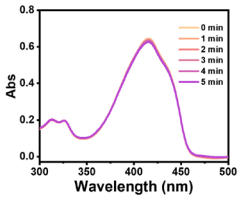

Figure S29. $^1O_2$ generation of DMF illuminated by 808 nm laser (1.0 W cm^{-2}) using 1,3-diphenyliso-benzofuran (DPBF) as an indicator.

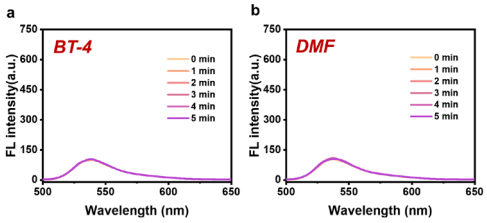

Figure S30. •O_2^- generation of **BT-4** (10 μM) (a) and DMF (b) illuminated by 808 nm laser (1.0 W cm^{-2}) using Dihydrorhodamine 123 (DHR123) as an indicator.

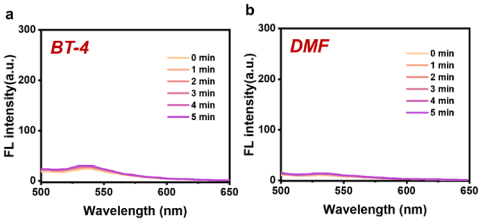

Figure S31. •OH generation of **BT-4** (10 μM) (a) and DMF (b) illuminated by 808 nm laser (1.0 W cm^{-2}) using Hydroxyphenyl Fluorescein (HPF) as an indicator.

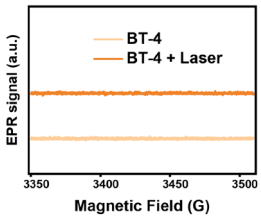

Figure S32. EPR spectra of **BT-4** (20 μM) under 808 nm irradiation (1.0 W cm^{-2}) for 5 min with DMPO as capture probes.

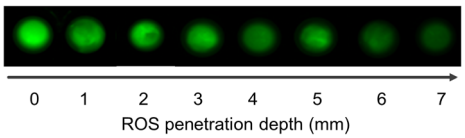

Figure S33. The DCF fluorescence imaging of **BT-4** (10 μM) at various depths.

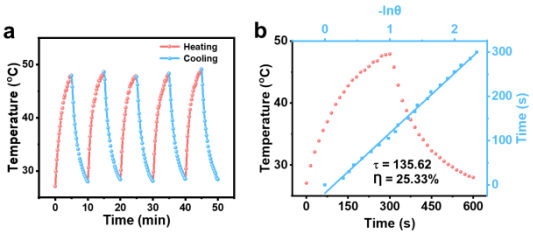

Figure S34. (a) Photothermal heating and natural cooling cycles for **BT-4** (20 μM) in DMF under

808 nm laser irradiation (1.0 W cm^{-2}). (b) Heating and natural cooling curve and corresponding linear time versus -lnθ data of **BT-4** (20 μM) in DMF under 808 nm laser irradiation (1.0 W cm^{-2}).

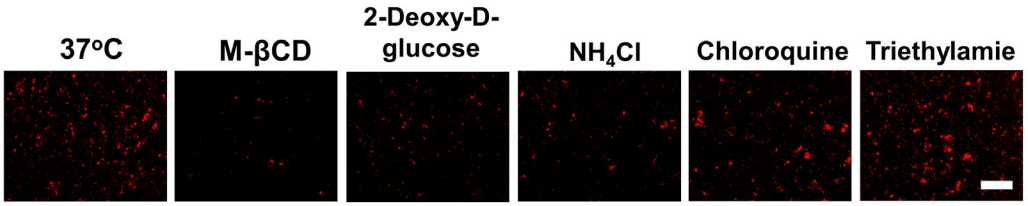

Figure S35. Cell uptake mechanistic study of **BT-4** (10 μM) in the presence of different inhibitors/conditions. Scale bar: 300 μm.

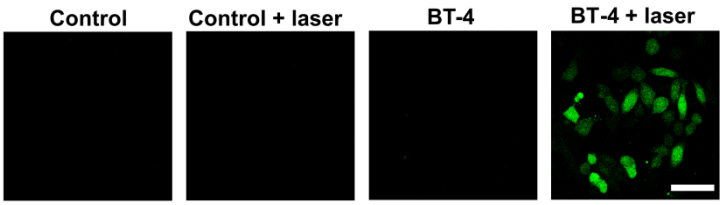

Figure S36. Inverted fluorescence microscope images of 4T1 cells incubated with DCFH-DA under various treatments. Scale bar: 50 μm.

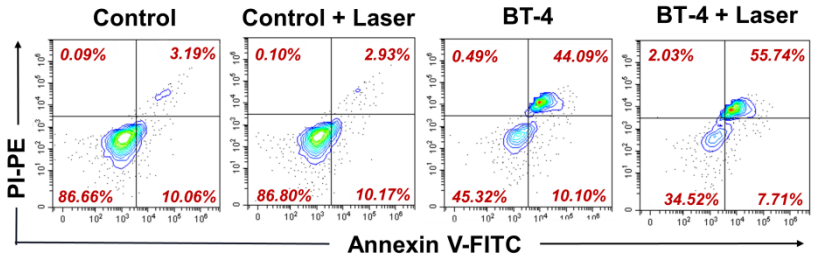

Figure S37. Flow cytometry test of Annexin-V-FITC/PI double-staining of 4T1 cells under different treatments.

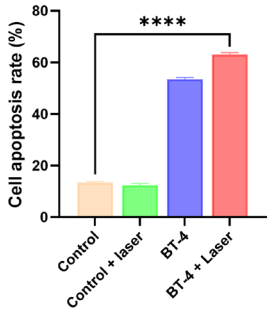

Figure S38. Quantitative comparison of total cell apoptosis rate. The data are presented as the mean±SD (n=3). ****p<0.0001

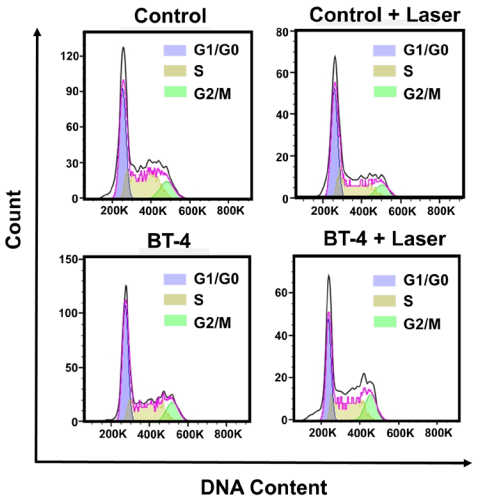

Figure S39. Cell cycle analysis of 4T1 cells by flow cytometry after different treatments: Control, Control + Laser (808 nm, 1.0 W cm^{-2}, 5 min), **BT-4**, and **BT-4** + Laser, respectively.

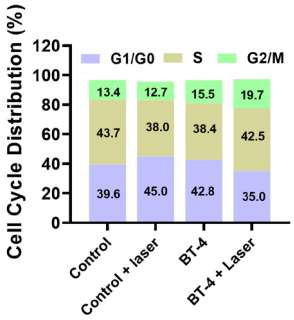

Figure S40. Histogram depictingcell population in the cell cycle stages after various treatments.

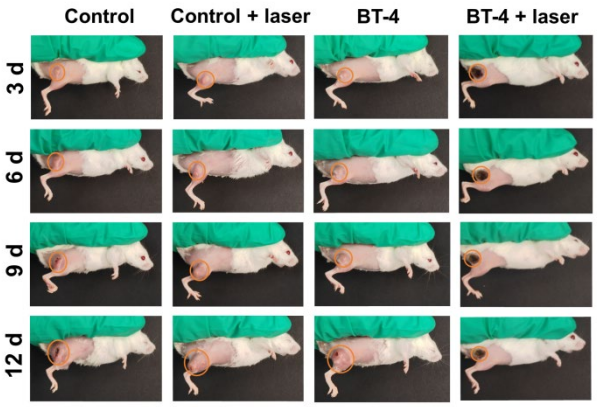

Figure S41. Bright images of mice treated with the indicated formulations at 3, 6, 9 and 12 days.

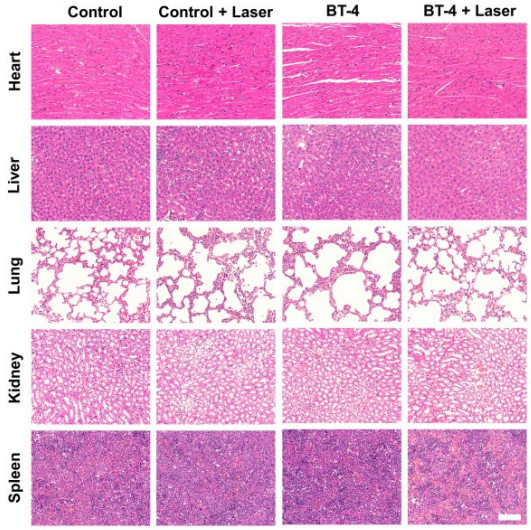

Figure S42. H&E staining of major organs including the heart, liver, spleen, lungs and kidneys of mice treated with different formulations (Control, Control + laser, **BT-4** and **BT-4** + laser). Scale bar: 100 μm.

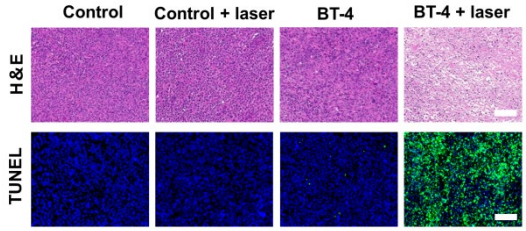

Figure S43. H&E and TUNEL staining of tumor slices collected from tumor mouse models. Scale bar: H&E, 100 μm; TUNEL, 100 μm.

4. Supplementary Tables

	Dark	Light	PI[a]
BT-4	32.3 ± 4.4	9.5 ± 2.0	3.4
ICG	338.3±5.5	5.6±1.1	60.3

Table S1. IC_{50} value of **BT-4** against 4T1 cells.

[a] PI (Photocytotoxicity Index) = $IC_{50,\,dark}$ / $IC_{50,\,light}$

5. Supplementary References

S1. L. Tu, C. Li, Q. Ding, A. Sharma, M. Li, J. Li, J. S. Kim, Y. Sun, *J. Am. Chem. Soc.* 2024, **146**, 8991-9003.

S2. C. Li, L. Tu, Y. Xu, M. Li, J. Du, P. J. Stang, Y. Sun, Y. Sun, *Angew. Chem. Int. Ed.* 2024, **63**, e202406392.